



My Pillow Knows My Sleep: Sleep Monitoring with Computational Fabrics in the Pillowcase

QIJIA SHAO, The Hong Kong University of Science and Technology, China

JUNXIAO CHEN, The Hong Kong University of Science and Technology; Tsinghua University, China

HO MAN COLMAN LEUNG, Columbia University, USA

MEIQI ZHAO, Columbia University, USA

RUOYU XU, Columbia University, USA

JITING LIU, The Hong Kong University of Science and Technology, China

LISA MARIA DISALVO GARCÍA, Columbia University, USA

XIAOFAN JIANG, Columbia University, USA

MARIE-PIERRE ST-ONGE, Columbia University, USA

XIA ZHOU, Columbia University, USA

Sleep is a vital physiological state that significantly impacts overall health. Continuous monitoring of sleep posture, heart rate, respiratory rate, and body movement is crucial for diagnosing and managing sleep disorders. Current monitoring solutions often disrupt natural sleep due to discomfort or raise privacy and instrumentation concerns. We introduce PillowSense, a fabric-based sleep monitoring system seamlessly integrated into a pillowcase. PillowSense utilizes a dual-layer fabric design. The top layer comprises conductive fabrics for sensing electrocardiogram (ECG) and surface electromyogram (sEMG), while the bottom layer features pressure-sensitive fabrics to monitor sleep location and movement. The system processes ECG and sEMG signals sequentially to infer multiple sleep variables and incorporates an adversarial neural network to enhance posture classification accuracy. We fabricate prototypes using off-the-shelf hardware and conduct both lab-based and in-the-wild longitudinal user studies to evaluate the system's effectiveness. Across 151 nights and 912.2 hours of real-world sleep data, the system achieves an F1 score of 88% for classifying seven sleep postures, and clinically-acceptable accuracy in vital sign monitoring. PillowSense's comfort, washability, and robustness in multi-user scenarios underscore its potential for unobtrusive, large-scale sleep monitoring.

CCS Concepts: • Human-centered computing → Ubiquitous and mobile computing systems and tools; • Applied computing → Health care information systems; • Hardware → Sensor devices and platforms.

Additional Key Words and Phrases: sleep monitoring, ECG, sEMG, conductive fabrics, heart rate, respiratory rate

Authors' addresses: Qijia Shao, The Hong Kong University of Science and Technology, Hong Kong SAR, China, qjiashao@ust.hk; Junxiao Chen, The Hong Kong University of Science and Technology; Tsinghua University, China, jchenjy@connect.ust.hk; Ho Man Colman Leung, Columbia University, USA, colman.leung@columbia.edu; Meiqi Zhao, Columbia University, USA, mz2651@columbia.edu; Ruoyu Xu, Columbia University, USA, rx2241@columbia.edu; Jiting Liu, The Hong Kong University of Science and Technology, China, jitingliu@ust.hk; Lisa Maria DiSalvo García, Columbia University, USA, ld3126@columbia.edu; Xiaofan Jiang, Columbia University, USA, JIANG@ee.columbia.edu; Marie-Pierre St-Onge, Columbia University, USA, ms2554@cumc.columbia.edu; Xia Zhou, Columbia University, USA, xia@cs.columbia.edu.

Permission to make digital or hard copies of all or part of this work for personal or classroom use is granted without fee provided that copies are not made or distributed for profit or commercial advantage and that copies bear this notice and the full citation on the first page. Copyrights for components of this work owned by others than the author(s) must be honored. Abstracting with credit is permitted. To copy otherwise, or republish, to post on servers or to redistribute to lists, requires prior specific permission and/or a fee. Request permissions from permissions@acm.org.

© 2025 Copyright held by the owner/author(s). Publication rights licensed to ACM.

ACM 2474-9567/2025/9-ART128

<https://doi.org/10.1145/3749550>

ACM Reference Format:

Qijia Shao, Junxiao Chen, Ho Man Colman Leung, Meiqi Zhao, Ruoyu Xu, Jiting Liu, Lisa Maria DiSalvo García, Xiaofan Jiang, Marie-Pierre St-Onge, and Xia Zhou. 2025. My Pillow Knows My Sleep: Sleep Monitoring with Computational Fabrics in the Pillowcase. *Proc. ACM Interact. Mob. Wearable Ubiquitous Technol.* 9, 3, Article 128 (September 2025), 26 pages. <https://doi.org/10.1145/3749550>

1 INTRODUCTION

Sleep is a naturally recurring state essential for human health. High-quality sleep is critical for achieving and maintaining cardiovascular health [70], for learning and memory consolidation [85], and for regulating emotions and overall well-being [35, 45, 61]. As shown in prior medical studies [8, 12, 32, 50, 54, 75, 97, 107, 114], sleep quality is directly correlated to various sleep variables such as sleep posture, vital signs, and body movement. As examples, improper sleep postures can lead to exacerbation of chronic diseases such as obstructive sleep apnea [50, 75, 97] and Parkinson's disease [77]; vital signs such as heart rate (HR) and respiratory rate (RR) provide critical insights into sleep conditions and can be used to detect sleep disorders [9, 18, 19, 44, 46, 71, 96, 100, 103]; along with body movement, these sleep variables can be used to infer sleep stages, providing a comprehensive approach to sleep monitoring [5, 11, 16].

Phenotyping sleep health appropriately and reliably across populations requires tools that are accurate and accessible. Most existing technologies rely on on-body devices worn on the wrist (e.g., FitBit, Actigraph, Garmin, Apple watch), finger (e.g., Oura ring), or head [40, 60, 89]. Some individuals can be sensitive to devices on their bodies, which disturbs sleep. Other populations, such as young children and individuals with mental disorders, are unable to tolerate these devices, precluding appropriate sleep assessments [34, 86]. Furthermore, existing wearable devices are unable to monitor sleep poses. Recent research has explored device-free methods using acoustic or radio-frequency signals (e.g., Wi-Fi) [15, 38, 61, 62, 90, 95, 123, 124]. While technically exciting, these methods are susceptible to ambient interference. It is also challenging to scale them up to reliably monitor multiple co-sleeping users. Additionally, camera-based monitoring methods raise privacy concerns [23].

In this paper, we propose a different approach to home-based sleep monitoring, which embeds soft fabric sensors into everyday pillowcases to simultaneously sense multiple sleep variables (e.g., poses, vital signs, body movement). The choice of these variables is guided by their importance in the early detection of sleep disorders and their relevance to general wellness monitoring. Existing research on smart pillows [3, 56, 59, 113] explores various solutions for sleep quality monitoring. However, many of these approaches rely on rigid sensors embedded in pillows or require additional wearable devices, potentially disrupting the user's sleep experience and limiting their practicality for daily use. Our proposed fabric sensors are made of off-the-shelf, soft conductive fabrics, which serve as sensing electrodes to measure the electrocardiogram (ECG) and surface electromyography (sEMG) around the sleeper's neck. Our approach eliminates the need for the user to wear any on-body sensor and relies on the natural contact between the user's neck skin and pillowcase fabric to monitor sleep. It also eliminates the need for significant alterations to the bedroom environment with minimal instrumentation. This ensures that users experience no difference in sensation compared to their usual sleep routine, which is crucial for encouraging user acceptance for long-term use. Furthermore, the ubiquity of pillows (used by over 98% of individuals) ensures widespread applicability, making our system accessible to a broad spectrum of users.

Realizing this approach presents several challenges. They include the uncertainty of the neck contact location on the pillow, the weakness of ECG and sEMG signals that inherently interfere with each other, the challenge of inferring whole-body postures purely based on physiological signals sensed around the neck, as well as user variations. We address these challenges in PillowSense. PillowSense employs a design of a fabric sensor array that integrates a biopotential sensing layer consisting of conductive fabric sensor patches and a pressure sensing layer with an array of pressure fabrics. It senses the neck contact location and activates only the biopotential sensor patches at the contact location to save power while maintaining the sensing frame rate. We also develop

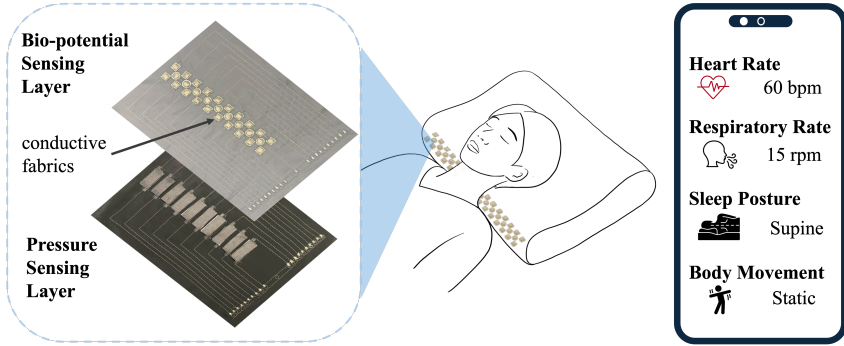


Fig. 1. PillowSense measures neck-based ECG and sEMG with sensing fabrics in a pillowcase and infers multiple clinically-meaningful sleep variables concurrently.

algorithms to fuse ECG and sEMG signals for inferring multiple sleep variables and apply adversarial learning for extracting user-independent features and dealing with user diversity. We fabricate multiple PillowSense prototypes using off-the-shelf hardware and evaluate the system through a lab study with 20 participants and a longitudinal deployment involving 21 participants across 151 nights. We summarize our key findings as below:

- PillowSense classifies four main sleep poses (left, right, supine, and prone), with an F1 score of 97% in the lab study and 91% in the longitudinal study using a generic model with leave-one-user-out cross-validation. The adversarial learning module substantially enhances generalization for all seven poses, improving the F1 score from 75% to 83% in the lab study and reaching 88% in the longitudinal study.
- PillowSense attains an average F1 score of 92% in classifying all seven postures using a personalized model trained with only seven minutes of data from each user, showcasing its capability for effective sleep posture classification with minimal training.
- PillowSense accurately estimates HR and RR in both controlled and natural sleep environments, achieving mean absolute errors of 2.5/2.7 bpm for HR and 2.4/3.1 rpm for RR in lab/longitudinal studies respectively, when compared to an FDA-approved pulse oximeter. Comparison to Apple Watch, an example consumer-grade wearable device, shows comparable accuracy results.
- PillowSense detects movement during sleep, maintains sensing performance across multiple co-sleeping users, remains robust against sanitization and repeated washing, and is consistently rated highly by participants for its comfort and usability after extended, real-world usage.

2 SENSING RATIONALE

We aim to simultaneously sense three sleep variables that are clinically meaningful for sleep monitoring: 1) sleep posture, 2) vital signs including HR and RR, and 3) body movement. Specifically for sleep postures, we seek to classify seven most common sleep postures (Figure 2), including (a) supine (lying on the back), (b) prone (lying face down), (c) left lateral (lying on the left side), (d) right lateral (lying on the right side), (e) left fetal (curled up on the left side), (f) right fetal (curled up on the right side), and (g) hooking (curled up on the back). These postures are extensively documented in prior research [10, 22, 88, 118]. Each posture is known to affect physiological processes and has potential health implications [16, 22, 88]. Among these, supine and lateral postures directly affect lung volume and upper airway patency, playing a critical role in conditions such as obstructive sleep apnea (OSA) and hypopneas [50, 75, 97]. In gastroesophageal reflux disease (GERD), the right lateral position is associated with increased reflux, while the left lateral position significantly reduces nocturnal acid exposure [107]. Leg positioning also impacts sleep quality. Side-lying positions with legs bent above 45 degrees offer greater stability and comfort for prolonged sleep [54]. Individuals with neck pain often adopt twisted side postures with

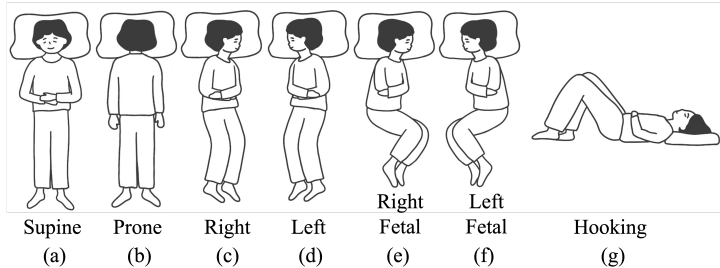


Fig. 2. Seven most common sleep postures.

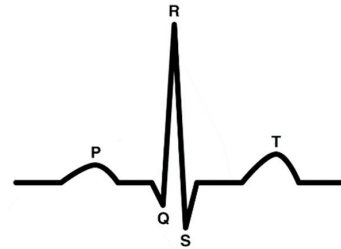


Fig. 3. ECG signal waveform [43].

misaligned legs, contributing to spinal rotation, muscle spasms, and decreased sleep quality [12, 114]. Conversely, chronic low back pain patients may find supine positions uncomfortable unless knees are bent [8]. Understanding these effects is essential for assessing sleep health and developing personalized posture-based interventions to improve overall well-being.

Our sensing rationale capitalizes on the observation that these three sleep variables result in varying neck contact positions on the pillow and produce distinct patterns of biopotential signals around the neck. Specifically, we sense two types of biopotential signals – ECG and sEMG – on the neck to infer the sleep variables. Similarly to a prior work [105], we employ a fabric approach to sensing biopotential signals. Next we will provide a primer on ECG and EMG before elaborating on the sensing rationale.

ECG and EMG Primer. ECG and EMG are biopotential signals that record the human body's electrical activities associated with heart and muscle function, respectively. ECG is the electrical potentials generated by the depolarization and repolarization of cardiac cells, helping assess cardiac function and detect abnormalities [26]. It measures the electric currents produced as the heart muscle cells depolarize during each heartbeat. Typically, the frequency range of ECG signals is between 0.05 to 150 Hz, with most of the signal concentrated in the 0.05–35 Hz range [117]. A commonly used term in ECG analysis is the R-peak, which marks the highest point of the QRS complex, representing ventricular depolarization. As shown in Figure 3, the QRS complex consists of three distinct waveforms (i.e., P, QRS, T) that reflect the heart's electrical activity during each heartbeat. The interval between consecutive R-peaks indicates the heart rate, offering a direct measure of heartbeat frequency.

EMG measures the electrical activity produced by skeletal muscles, providing insights into neuromuscular health and muscle function. It captures electrical signals generated when motor neurons transmit impulses to muscle fibers that reflect muscle activity. The frequency of EMG signals ranges from 6 Hz to 500 Hz, with the highest spectral power between 20 Hz and 150 Hz, depending on the type of muscle activity being monitored [55, 110]. Surface EMG (sEMG) involves placing electrodes on the skin overlying muscles to detect the motor unit potentials that reflect muscle activity during motion or static conditions [28, 39, 74]. sEMG signals are employed to assess muscle activation patterns, evaluate muscle fatigue, and diagnose neuromuscular disorders.

Fabric Sensing of Neck Biopotential Signals. Traditional ECG measurements place electrodes on the chest and/or limbs [26], which restricts movement and disrupts natural sleep patterns. Through our experiments, we discovered that ECG signals can also be measured from the neck. Specifically, we conducted a controlled experiment involving four participants. We fabricate four pairs of fabric sensors made of conductive fabrics to serve as electrodes for a one-lead ECG sensing, simultaneously positioning them at four locations on the neck, i.e., the front, back, left, and right of the neck (Figure 4(a)). Additionally, conventional adhesive electrodes are attached to each participant's hands to collect standard lead-I ECG signals as the ground truth.

Figure 4(a) plots the ECG measured by each sensor pair with a bandpass filter of 5 Hz to 50 Hz. We obtain two key observations. (1) Although the waveform of the ECG signals sensed by the fabric sensors differ from the

ground truth ECG, the R-peak locations are consistently identical and synchronized across all measurements. The discrepancy in waveform shapes is attributed to sensor placement. Different sensor locations/leads yield distinct ECG waveform characteristics [26, 76]. The synchronized R-peaks confirm the feasibility of obtaining accurate ECG readings from the neck with the conductive fabrics. (2) The variation of ECG signal characteristics when the electrodes are contacting different neck regions provides the basis for distinguishing various sleep postures.

We also validate the capability of fabric sensor for sensing neck sEMG. Since the measurement circuitry for ECG and sEMG is the same, we can extract sEMG using a different bandpass filter (50 Hz to 125 Hz), based on the biopotential signals sensed by the same set of fabric sensors used for ECG measurements. In the experiment, participants are instructed to tilt their heads multiple times to record sEMG signals. As shown in Figure 4(b), sEMG signals sensed by fabric sensors on the neck exhibit higher amplitudes during neck movement when neck muscles are activated. It aligns with the literature [49, 109] and confirms the viability of measuring neck sEMG with fabric sensors contacting the neck.

Together, these experimental observations motivate us to embed fabric sensors into the pillowcase, where fabric sensors can sense ECG and sEMG signals at the contact neck region during sleep. Various sleep poses lead to different neck regions in contact and distinct patterns of ECG and sEMG signals. It forms the basis for inferring various sleep variables and enables a comfortable and noninvasive method for sleep monitoring without requiring any on-body sensors.

Challenges. Transitioning this concept into a practically deployable system presents several challenges. First, maintaining consistent contact between the fabric sensor and neck skin is challenging, as movement during sleep is common. Importantly, we aim to avoid using adhesives on the human body to preserve natural sleep patterns, which complicates stable sensor placement. Second, ECG signals detected at the neck, especially on the lateral sides, are notably weak, presenting a challenge in obtaining high-quality data. Amplifying these signals to achieve a high signal-to-noise ratio (SNR) without introducing significant noise or artifacts is non-trivial. Moreover, since the ECG and sEMG have overlapping frequency ranges, they could interfere with each other, appearing as noises. Third, ECG and sEMG reflect distinctly different body activities. Effectively fusing these signals to collectively provide complementary information on sleep posture is complex. Finally, as shown in the previous experiments, signal variations when electrodes are positioned on different neck regions depend also on amplitude changes (e.g., left and back), which can fluctuate due to varying skin conditions and individual differences. Developing an algorithm that can adapt to these variations and generalize across different conditions is challenging.

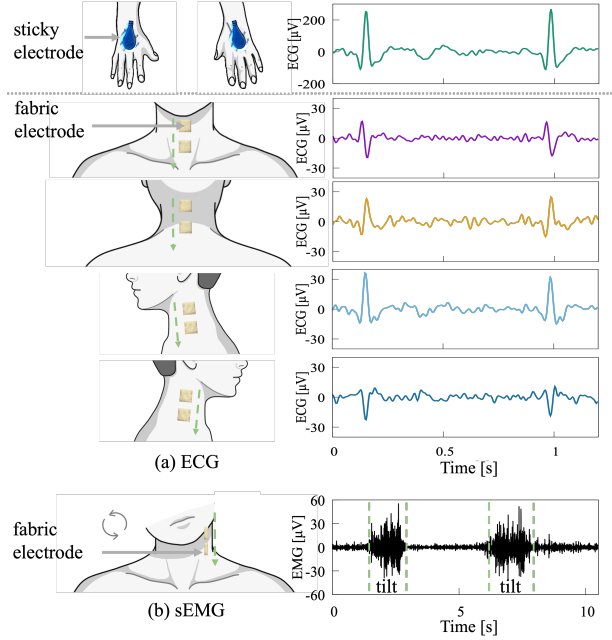


Fig. 4. The experimental setup for measuring the (a) ECG and (b) sEMG on the neck and the measurement results.

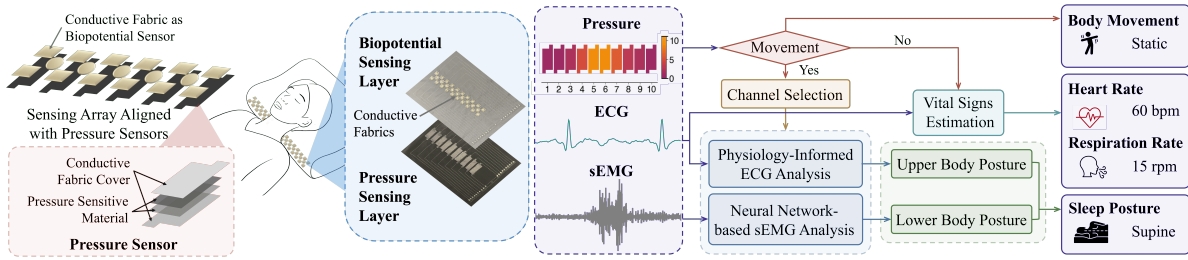


Fig. 5. PillowSense system overview.

3 PILLOWSENSE DESIGN

To overcome the above challenges, we design PillowSense. It consists of four primary design elements: (1) An array of fabric sensors that can be easily embedded into a pillowcase to capture ECG and sEMG signals from multiple directions on the neck. (2) An integration with pressure-sensitive fabrics provides users with the flexibility to sleep in any position on the pillow, adapting to the user's movements. (3) Implementation of a fusion algorithm that sequentially utilizes ECG and sEMG signals for sleep posture classification. (4) Development of an adversarial neural network that identifies features independent of user variations and generalizes the system better across diverse users. Figure 5 demonstrates the fabric array design and the system overview. Next, we detail the design components of our system in hardware and software aspects.

3.1 Design of Fabric Sensor Array

The proposed fabric sensor array comprises two layers: a biopotential sensing layer and a pressure sensing layer. The biopotential sensing layer is used to capture the ECG and sEMG signals, and the pressure sensing layer is used to detect which region the user is sleeping on and activate the corresponding biopotential sensing unit.

Biopotential Sensor Patch. As shown in Figure 6(a), the primary direction of ECG transmission in the heart, known as the heart axis, extends from the top right to the bottom left. The alignment between the heart axis and the measurement direction influences both the amplitude and orientation of the ECG signals [26]. Utilizing this physiological insight, we propose a sensor patch configuration to record biopotentials from multiple directions simultaneously. As depicted in Figure 6(b), each patch consists of four conductive fabric nodes arranged into six channels categorized into three types (two vertical, two horizontal, and two diagonal). To enhance the contact between the fabric and the skin, each sensor node is designed to be concave by placing kinesiology tape behind it. Further details on fabrication are provided in § 4.

Experimental results validate that the orientation of measurement channels significantly affects the SNR. As shown in Figure 6(c), the resultant ECG signals vary in shape and direction, although the R-peak locations remain synchronized. The optimal ECG recording is achieved via the diagonal channel (channel 6) in the supine posture, which aligns with the heart axis direction, yielding the highest amplitudes, while the perpendicular channel (channel 5) captures minimal ECG. Given the overlap of sEMG and ECG frequency bands, with ECG potentially acting as noise in sEMG measurements, our patch design leverages channels with minimal ECG interference for sEMG recordings. This approach effectively isolates ECG noise, enhancing sEMG signal clarity. Simultaneous sEMG measurements at six channels/directions also provide information on different muscular activities for inferring sleep postures.

Integration with Pressure Fabrics. Given that a sleeper moves during sleep and the neck can rest on different regions of the pillowcase, the array of biopotential sensor patches should cover the whole length of the pillow. However, this broad sensor coverage introduces the need to either monitor all biopotential patches simultaneously or sequentially sense them individually. Simultaneous monitoring, while comprehensive, is highly

power inefficient since most sensor patches are not in contact with the sleeper’s neck and thus are not actively engaged in signal measurement. On the other hand, sequentially cycling through the patches, although conserving power, largely reduces the sampling rate. This reduction can lead to the loss of high-frequency information, which is vital for accurate capture of sEMG data.

To address these issues, we have integrated a layer of pressure-sensitive fabrics beneath the biopotential sensing layer, each composed of a piezoresistive film sandwiched between two layers of conductive fabric, as depicted in Figure 5. Upon application of pressure, the resistance of this film shifts dramatically – from several mega-ohms to just a few hundred ohms. After exploration, we found that accurately differentiating sleep postures purely based on the pressure would require a significantly denser pressure sensor array. This would increase system complexity and power consumption. Therefore, we employ the pressure sensors primarily for localization and trigger functions. Although this simple and cost-effective setup cannot provide precise pressure measurements or detect subtle differences, it functions effectively as a switch when a resistance threshold is defined. This setup allows continuous sweeping through all channels to precisely identify the specific region that the user’s neck contacts. By aligning each pressure sensor with a corresponding column of biopotential sensors (Figure 5), we can selectively activate only those sensors located beneath the user. This selective activation conserves energy by powering down inactive sensors and maintains a high sampling rate essential for capturing biopotential signals. It is worth noting that, due to the high resistance of the pressure fabric in its idle state (several mega ohms), the matching resistance in the voltage divider circuit is similarly high. As a result, the total circuit resistance remains large all the time, keeping the current extremely low ($< 1\mu A$). Consequently, the heat generated by the circuit is negligible, ensuring safe and comfortable operation throughout use.

Furthermore, the pressure fabric array provides additional information on user movement, which is valuable for sleep staging [5, 94, 115] and can serve as a trigger for sleep posture classification. With the movement information, PillowSense activates posture classification only when the user stabilizes in a specific posture. Once posture classification is complete, the system waits until the next body movement and stabilization before activating the classification pipeline again. This approach conserves power and reduces computational demands, enhancing the overall efficiency.

3.2 Sleep Posture Classification

Utilizing collected ECG and sEMG, PillowSense adopts a sequential approach to posture classification. Initially, ECG data is analyzed to determine the upper body posture, categorizing it as left, right, supine, or prone. Lower body posture (i.e., leg bending), does not affect the ECG signals directly. But it does influence the amount of force exerted on the neck to maintain a particular posture (e.g., the hooking posture offloads the lower body weight from the neck, requiring less force to support it). These force variations are minimal, making them difficult to detect with standard pressure sensors. Therefore, sEMG data is subsequently employed to determine whether the legs are bent, hence differentiating all the seven sleep postures.

Physiology-Informed ECG Analysis. Given the heart’s frontal and central (slightly left) positioning within the chest, four surfaces of the neck (left, right, front, and back) offer unique perspectives of the heart’s electrical activity. Our system leverages six channels (Figure 6) of biopotential readings to analyze sleep postures.

Our experiments validate this theoretical insight by demonstrating a consistent pattern associated with the side of the neck contacting the biopotential sensor patch. We use the ECG’s R-peak amplitude to define the ECG signals’ directionality: If the R-peak amplitude in a measuring channel is positive, we define the ECG direction as positive; if it is negative, the direction is negative. As shown in Figure 7, when the left or right side of the neck is in contact, the six ECG channels display uniformly positive or negative directions, respectively. This uniformity across ECG channels is due to the channels’ consistent orientation relative to the heart’s position on either the left or right side of the neck. Conversely, when the front or back of the neck makes contact, the ECG

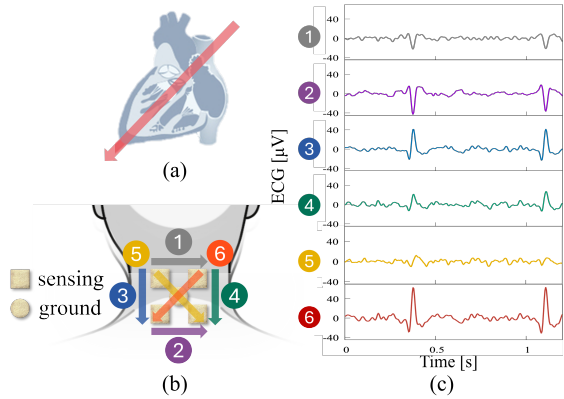


Fig. 6. (a) The heart axis is from the top right to the top left. (b) The sensing patch design forms 6 measurement directions. (c) ECG signals recorded by the proposed sensor patch on the back of the neck (supine posture).

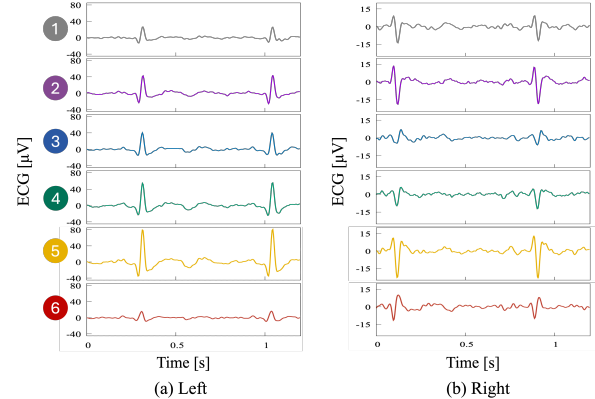


Fig. 7. (a) Sleeping on the left side results in all positive R-peaks, whereas (b) sleeping on the right side results in negative R-peaks.

signal directions in the six channels are different and show unique patterns. Taking the back side as an example, as illustrated in Figure 6(c), channels (3,4,6) that align with the heart's axis (vector angle less than 90 degrees) are positive, with channel 6 exhibiting the highest amplitude due to its optimal alignment. The remaining channels (1,2,5) are negative, with channel 5 displaying the lowest amplitude as it is the most perpendicular to the heart's axis. By analyzing the R-peak amplitudes across all six channels, we can determine which side of the neck is in contact with the pillow, thereby identifying whether a person is sleeping in a left, right, supine, or prone position.

This physiology-informed approach leverages fundamental aspects of human physiological structure to ensure broad applicability to most individuals, except those with atypical heart axes. It remains robust and unaffected by external environmental factors, making it generalizable and suitable for multi-user scenario.

User-Independent sEMG Analysis. Once the upper body posture of the user is determined, the next step is to detect whether they are bending their legs. Similar to previous research [58, 91, 101], our experiments showed that lower body movements influence neck muscle activities during sleep. These differences manifest primarily in the amplitude of the sEMG signals measured on the neck. However, the amplitude can be affected by various factors, including the point of contact, skin condition, and skin type, making it challenging to establish a universal threshold applicable to all users for detecting leg bending. Consequently, we propose a neural network-based approach, which consists of three main modules: a feature extractor, a leg-bending detector, and a user discriminator. As shown in Figure 8, the feature extractor first extracts leg-specific representations separately and fuses information between different directions together. The learned joint representation is then fed to the leg-bending detector. To ensure the learned joint representation contains little user-specific information, we add a user discriminator module for better cross-user performance. Next, we explain each module in detail.

Feature Extractor. The raw sEMG signals are first processed using a bandpass filter ranging from 50 Hz to 125 Hz and a 60 Hz notch filter to eliminate power line noise. We then segment the sEMG signals into three pairs of two-channel configurations: horizontal, vertical, and diagonal, to capitalize on the spatial distribution of the signals. For input processing, we opt for a window size of 4 seconds with a 1-second moving step. Following the methodology similar to EEGNet [57], the data undergo three sequential convolutional steps. Initially, the sEMG data are subjected to a 2D convolutional neural network (2D-CNN), extracting meaningful temporal features. Subsequently, a depth-wise convolution layer [17] is employed to learn spatial filters effectively. A subsequent 2D-CNN is applied to refine the temporal features of each spatial filter. After processing, three feature vectors

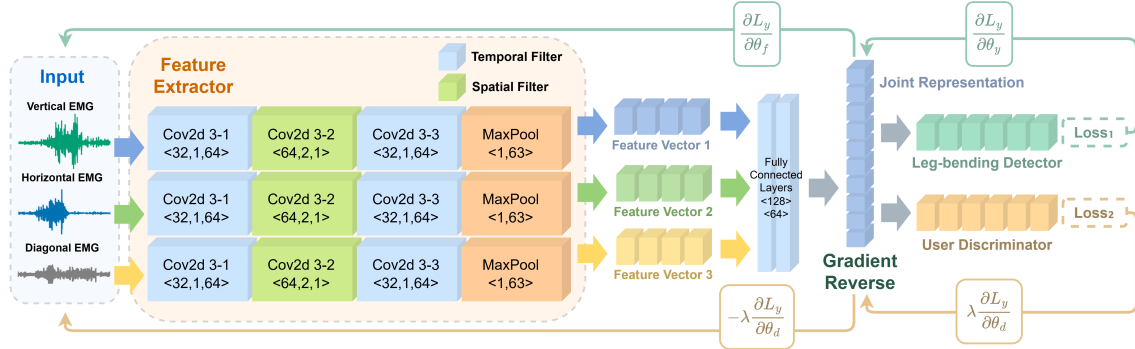


Fig. 8. The network architecture incorporates backpass-filtered sEMG signals from three directions as inputs. The hyperparameters of Conv2d are shown as $<channel, kernel_x, kernel_y>$; The max-pooling layer's kernel size is $<kernel_x, kernel_y>$; The fully-connected layer's hidden units size is $<size>$. The model is trained with an adversarial objective: a leg-bending detector predicts the target label, while a user discriminator—optimized via a gradient reversal layer—encourages the shared features to be user-invariant. This adversarial setup enhances cross-user generalization and enables better posture classification across different individuals.

are concatenated and then fed into two fully-connected layers. These layers integrate features from different channels, yielding a unified representation for the leg-bending detection and user discriminator modules.

Leg-bending Detector. The leg-bending detector module decides whether the user is bending their legs, operating as a binary classifier. This module comprises three sequentially stacked fully connected layers with hidden sizes of 64, 16, and 2, respectively. The final output layer employs a LogSoftmax function to calculate the probabilities of belonging to each class. The model utilizes weighted cross-entropy loss as the loss function, defined as:

$$Loss_1 = -\frac{1}{N} \sum_{k=1}^N \frac{\sum_{i=1}^M W_i \log(\frac{\exp x_{k,i}}{\sum_{j=1}^M \exp x_{k,j}})}{\sum_{i=1}^M W_i}, \quad (1)$$

where W_i , N , and M represent the weight of the i -th class, the total number of labeled samples, and the number of classes, respectively. Each class weight is inversely proportional to its frequency.

User Discriminator. We repurposed a domain adaptation technique [30] for supervised learning since user labels are available, aiming to extract user-independent features. The user discriminator module uses the joint representation as input, with the user index as the label to predict the user. This module consists of two fully connected layers with hidden sizes of 32 and 20/21 (the number of users). The loss function used is a cross-entropy function:

$$Loss_2 = -\frac{1}{N} \sum_{k=1}^N \sum_{i=1}^U \log(\frac{\exp x_{k,i}}{\sum_{j=1}^U \exp x_{k,j}}), \quad (2)$$

where N is the number of labeled samples and U is the number of users. Ideally, the user discriminator should exhibit low accuracy, indicating that the joint representation contains minimal user-specific information. To encourage this, we incorporate a gradient reversal layer [30]. This layer forwards the joint representation unchanged during the forward pass but inverts the gradient sign during backpropagation by multiplying it by a constant λ . The entire network is trained using a combined loss function defined as:

$$Loss = Loss_1 - \lambda * Loss_2 \quad (3)$$

This minmax game, which involves minimizing $Loss_1$ and maximizing $Loss_2$, ultimately converges to a saddle point, producing user-independent features [30, 51, 120].

3.3 Vital Sign Inference

Vital signs are inferred based on the ECG signals captured across six channels. Specifically, we first calculate the SNR for each channel and then select the one with the highest SNR to estimate HR and RR.

Heart Rate. To enhance the robustness and reliability of QRS detection in ECG signals, we implemented an Ensemble Empirical Mode Decomposition (EEMD)-based approach [116]. Specifically, given a raw ECG signal $x(t)$, the EEMD decomposition process can be mathematically represented as:

$$x(t) = \sum_{j=1}^n c_j(t) + r_n(t), \quad (4)$$

where $c_j(t)$ ($j = 1, 2, \dots, n$) denote the Intrinsic Mode Functions (IMFs), each representing distinct frequency components of the original signal, and $r_n(t)$ is the residual signal after extracting n IMFs. Typically, the second IMF, $c_2(t)$, is selected as it empirically contains the clearest representation of the QRS complex due to its frequency alignment with ventricular depolarization events [2]:

$$x_{\text{IMF}}(t) = c_2(t). \quad (5)$$

Next, we compute the instantaneous envelope of the selected IMF via the Hilbert transform, as follows:

$$e(t) = |x_{\text{IMF}}(t) + j\mathcal{H}\{x_{\text{IMF}}(t)\}|, \quad (6)$$

where $\mathcal{H}\{\cdot\}$ represents the Hilbert transform operation and $e(t)$ is the resulting envelope that accentuates the features of R-peaks. Subsequently, R-peak candidate positions p_k are identified by applying a peak-finding algorithm to the envelope signal $e(t)$, with a minimum inter-peak interval constraint T_{\min} :

$$\{p_k\} = \{t \mid e(t) \text{ is local maximum, } p_k - p_{k-1} \geq T_{\min}\}, \quad (7)$$

where we set $T_{\min} = 0.5$ s, reflecting physiological heart-rate limits (maximum 120 bpm). This constraint reduces false positives arising from noise and other ECG components such as the T-wave. Finally, precise R-peak positions R_k are refined by searching within a local interval around each candidate p_k in the original ECG signal $x(t)$:

$$R_k = \arg \max_{t \in [p_k - \delta, p_k + \delta]} x(t), \quad (8)$$

with δ representing a small search window chosen empirically (e.g., ± 50 ms) around the candidate positions. This step ensures that the detected peaks align accurately with true R-wave events. The instantaneous HR over the past 10 seconds is computed from the time intervals between consecutive R-peaks using the formula:

$$H = \frac{1}{\sum_{i=1}^{10} d_i / 10}, \quad (9)$$

where d_i represents consecutive R-peak intervals.

Respiration Rate. To estimate RR, we analyze the frequency modulation of the ECG, specifically the respiratory sinus arrhythmia, which reflects HR fluctuations during the breathing cycle—increasing during inhalation and decreasing during exhalation [7, 52]. We derive heart rate variability (HRV) from the HR data calculated earlier, which shows the variation in intervals between heartbeats. Applying a Fast Fourier Transform to HRV data, we locate the peak frequency within the typical respiration range (11-30 rpm), which represents the estimated RR.

4 PROTOTYPE IMPLEMENTATION

We fabricate multiple PillowSense prototypes using off-the-shelf hardware. We aim to not only optimize sensing performance, but also ensure its comfort and washability. Each prototype consists of micro-flex compression knit fabric pillowcases as the base layers, conductive fabrics as biopotential sensors, pressure-sensitive conductive fabrics as pressure sensors, conductive thread as wires, sports kinesiology tapes to insulate, flexible PCBs to

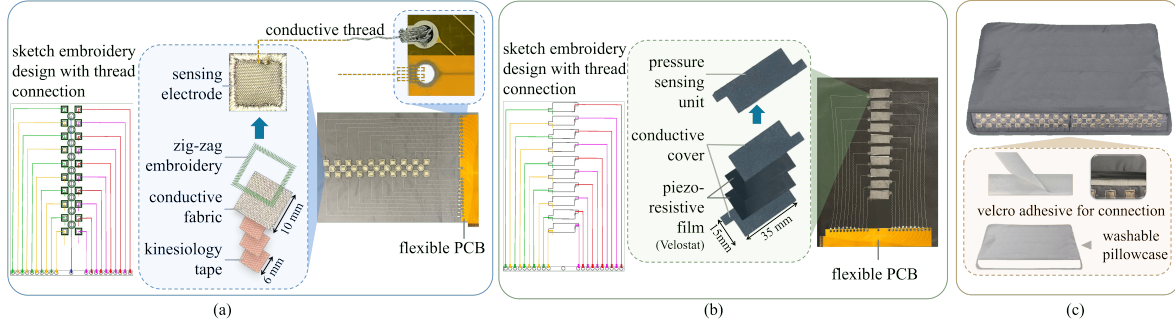


Fig. 9. Fabrication process of the biopotential sensing layer (a), the pressure sensing layer (b) and the final assembly (c).

connect, and two microcontrollers to process. All components are low-cost (<\$5), except for the computing units (\$499). Since our design is modular, it can be easily extended to arbitrary pillow sizes.

Biopotential Sensing Layer. The biopotential sensing layer consists of 10 fabric sensor patches arrayed horizontally on the pillowcase, each with four sensing electrodes and one ground electrode. Each sensing electrode is constructed from a layer of conductive fabric and three layers of kinesiology tape to increase electrode concavity for better skin contact (Figure 9(a)). The fabrication process consists of three main steps: (1) Utilizing a vector graphics editor [41, 93], we create a sensor layout tailored to the hoop dimensions of our embroidery machine [4]. The design incorporates rectangles as sensing electrodes and circles as ground electrodes, connected by lines representing conductive threads (Figure 9(a)). (2) The electrodes are constructed by stacking three 6 mm × 6 mm squares of kinesiology tape [31] to form a durable, concave base. Over this, a 10 mm × 10 mm square of conductive fabric [21], precisely cut with a Cricut machine [20], is applied. The assembly is then embroidered to maintain structural integrity and ensure optimal electrical functionality. (3) Each sensing electrode is connected to a flexible PCB by following the path specified in the Ink/Stitch file. Conductive threads [112] are carefully stitched and secured into the PCB's holes using a legacy fill stitch (Figure 9(a)).

Pressure Sensing Layer. The fabric pressure sensor employs a two-layer sandwich structure. We begin by cutting the piezoresistive film (Velostat) and conductive fabrics into precise dimensions (35 mm × 15 mm) using the Cricut machine. The piezoresistive film, slightly larger than the conductive fabric layers, is sandwiched between them to prevent direct contact. These components are then adhesively bonded to form an integrated pressure fabric. Two pressure fabric units are paired with a biopotential sensor patch and connected to the flexible PCB using similar embroidery stitches as that in the biopotential array shown in Figure 9(b).

Pillowcase Assembly. The final assembly involves sewing the biopotential sensing layer (top) and the pressure sensing layer (bottom) together, aligning the sensing units appropriately. The outer pillowcase is designed with an opening to expose the sensing units directly to the user's skin. For practical maintenance, the pillowcase is attached to the sensing layers using Velcro, facilitating straightforward detachment for cleaning purposes. Meanwhile, the sensing array itself can be sanitized using alcohol pads. The fully assembled prototype is depicted in Figure 9(c). The final pillow size is 21 inches by 14 inches.

Processing Units. A PCB was fabricated to interface with two flexible PCBs connected to the sensing layers (Figure 10). The pressure-sensitive fabric array is integrated using a 16-channel analog multiplexer [42], while the biopotential electrodes are connected through two 16-to-2 multiplexers [24]. An ESP32C3-based microcontroller [111] processes signals from the pressure fabric array and controls channel selection for the biopotential electrodes. The outputs from biopotential multiplexers are then fed into an OpenBCI Cyton board [82], configured to create six differential channels for biopotential sensing. The biopotentials, sampled at a rate of 250 Hz,

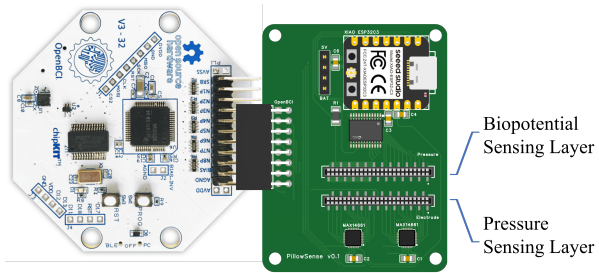


Fig. 10. The PCB design for the connection.



Fig. 11. The setup of the lab study.

are transmitted via Bluetooth Low Energy module to a MacBook Pro 2022 (M2 Max, 64GB) for further signal processing and inference. The whole system is embedded at the edge of the pillow to avoid interfering with sleep comfort. It is powered by a rechargeable battery which can be charged using a USB cable, allowing easy recharging without interrupting sleep use. We implemented the deep learning models in PyTorch and trained them on four NVIDIA RTX A1000 GPUs with a batch size of 64. Using an Adam optimizer, the learning rate started at 0.0005 and was halved every 10 epochs if validation accuracy did not improve. Training was capped at 100 epochs with an early stopping threshold of 30 epochs without improvement. The neural network's total parameter size is 4.08 MB.

5 SYSTEM EVALUATION

We evaluated PillowSense through two user studies, both approved by our Institutional Review Board (IRB). The first study was conducted in a controlled laboratory setting over a short duration, while the second was a longitudinal study conducted in the wild, lasting at least one week for each participant. Our evaluation focused on assessing sensing performance, usability, reliability in multi-user scenarios, and washability.

5.1 Study Setup and Data Collection

Lab Study. We recruited 20 healthy participants (7 males, 13 females, average age 24.2, age range 19-33). Each participant is compensated \$15 for completing the study. During the study, participants were instructed to remove any neck jewelry and tie up or move aside any long hair before positioning their necks on the pillow. As shown in Figure 11, participants slept on our prototype while wearing a pulse oximeter [73] on the index finger of their dominant hand. During the sessions, participants lay on the pillow with seven postures in Figure 2. To account for subtle variations in the same posture, each participant performed at least two rounds for each posture. In total, each posture was held for five to ten minutes. A blanket was available for additional comfort if necessary. The total duration of the study was around 1 hour for each participant. Upon completion, participants completed a user survey to provide feedback on their experience with the pillow. In total, we collected 1034 minutes of sleeping data, which was roughly evenly distributed across seven sleep postures. The lab study ensured data collection of all pre-defined postures from each participant, allowing us to systematically evaluate the sensing performance under consistent conditions while capturing posture-specific variations.

Longitudinal Study. To evaluate PillowSense in real-world natural sleep environments, we conducted another longitudinal study. In this study, each participant replaced their regular pillow with the PillowSense prototype for at least one week (7 nights). A total of 21 healthy participants¹ were recruited (12 males, 9 females; average age 23.7, age range 20-38). To investigate potential influencing factors, we recruited participants with diverse

¹Data from one participant who discontinued after a single night due to personal reasons was excluded from the analysis.

Table 1. Information of participants in the longitudinal study.

Category	Value	Details
# of Participants (n)	21	12 males, 9 females
Age (years old)	23.7 (avg)	Range: 20–38 years
Data Collected	151 nights	1025.1 hours sleep duration
Hairstyle (n)		
	8	Straight short hair (above neck)
	3	Curly short hair (above neck)
	6	Straight long hair (below neck)
	4	Curly long hair (below neck)
Neck Circumference (cm)	34.6 (avg)	Range: 27–41 cm
Nape Hair	6 Yes, 15 No	Self-reported
Sleep Sweating	3 Yes, 18 No	Self-reported

hairstyles and neck circumference (average 34.6 cm, range 27–41 cm). Participants were asked to report if they experience excessive sweating during sleep. We summarize participant information in Table 1.

Participants were instructed to use the pillow naturally, following their usual sleep habits. They were asked to remove any neck jewelry and to tie up or reposition long hair to ensure proper sensor contact before sleeping. To collect the ground truth of sleep poses, an infrared camera was deployed to record the sleep process continuously. Participants were given the option to use either an Apple Watch or a chest band as a reference device for vital sign monitoring; all participants preferred the Apple Watch over the chest band. Upon completion, participants also completed a user survey to provide feedback on their experience with the pillow.

In total, we collected 151 nights comprising 1025.1 hours of sleep. After aligning the data with the ground truth references, we obtained 912.2 hours across the same 151 nights in which the ground truth recordings were available. The remaining 103.9 hours of unusable data were excluded due to either the pulse oximeter falling off during sleep (82.3 hours) or disconnection of the ground truth camera system (21.6 hours).

Ground Truth and Evaluation Metrics. The ground truth of sleep poses and body movement was obtained through manual observation in the lab study and via video recordings in the longitudinal study. HR and RR ground truth data were collected using an FDA-approved device [73]. The accuracy of this device is reported with a mean absolute error (MAE) of 3 beats per minute (bpm) for HR and 2–4 respirations per minute (rpm) for RR [72]. In real-world use, posture classification is triggered only when the user stabilizes in a specific posture and remains inactive until a new movement is detected by the pressure sensors. However, for evaluation purposes, we continuously classified non-overlapping four-second segments into one of seven predefined postures, assessing performance using weighted recall, precision, and their harmonic mean (i.e., F1 score). The accuracy of HR and RR sensing was evaluated using MAE. Additionally, heart rate measurements from the Apple Watch, recorded via the Heart Graph app, were used as a supplementary reference for comparison.

5.2 Posture Classification Performance

5.2.1 Generic Model. To assess the generalizability of our method, we utilize a leave-one-user-out cross-validation approach for posture classification.

Lab Study Results. In the controlled lab study, PillowSense demonstrated strong classification performance. As shown in Fig. 12 (a), it achieved an F1 score of 97% for upper body posture detection (i.e., supine, left, right, and prone), and an F1 score of 82% for leg bending detection, confirming the effectiveness of utilizing neck EMG signals for lower body movement inference. The overall F1 score for classifying all seven postures was 83%. Disabling the adversarial training module led to an 8% decrease in performance, underscoring its importance in enhancing cross-user generalization.

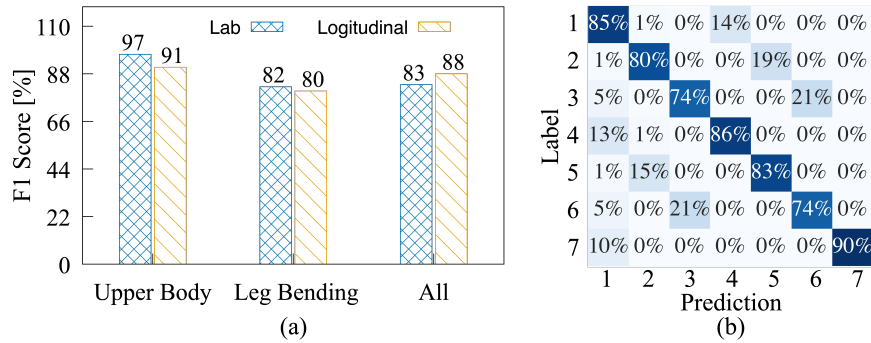


Fig. 12. Results of leave-one-user-out cross-validation. (a) posture classification performance for both studies and (b) confusion matrix on the classification accuracy across all postures in the lab study: 1 Supine, 2 Left, 3 Right, 4 Hooking, 5 Left Fetal, 6 Right Fetal, 7 Prone.

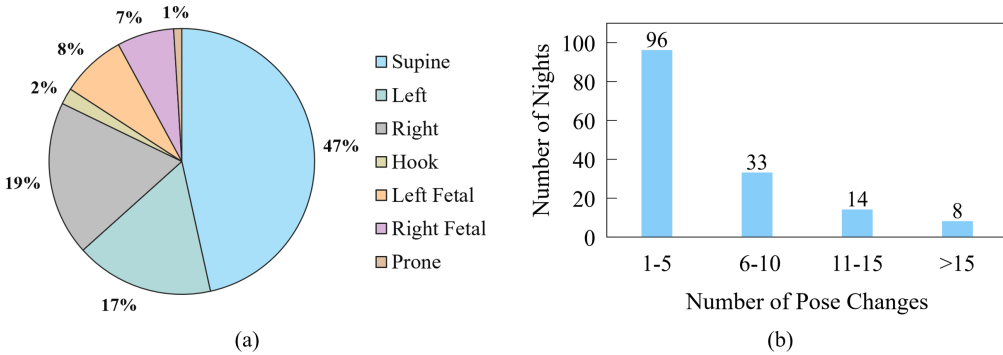


Fig. 13. Distribution of (a) collected sleep poses and (b) the number of overnight pose changes in the longitudinal study.

Longitudinal Study Results. In the longitudinal study, participants slept naturally without any posture constraints. This resulted in a highly uneven distribution of sleep postures, as detailed in Fig. 13(a). Additionally, we recorded the frequency of posture changes during overnight sleep (Fig. 13(b)). The majority of participants changed their sleep poses fewer than five times per night, with some maintaining only one or two postures throughout the entire sleep period.

An additional challenge observed in the real-world setting was intermittent loss of contact between the neck and the pillow, as indicated by the pressure sensor readings. Out of the total 912.2 hours of recorded data, 71.2 hours (approximately 7.8%) were identified as data loss. Video reviews revealed that 3.8% of this loss occurred when participants were physically in contact with the pillow but experienced poor sensor contact, likely due to movement or hair blockage, while the remaining 4% resulted from participants not being in contact with the pillow at all. This reveals a limitation of the current prototype, where consistent contact between the neck and fabric sensors cannot always be maintained due to natural user movements and variations in hair coverage. Potential strategies to address this limitation are discussed in §6.

For evaluating pose classification performance, these periods of data loss were excluded from analysis. Despite variability in pose distribution, PillowSense achieves an F1 score of 91% for upper body posture detection and 80% for leg bending detection (Fig. 12(a)). The overall F1 score for classifying seven postures reached 88%, slightly higher than in the lab study, primarily due to the predominance of non-leg-bending postures in the longitudinal

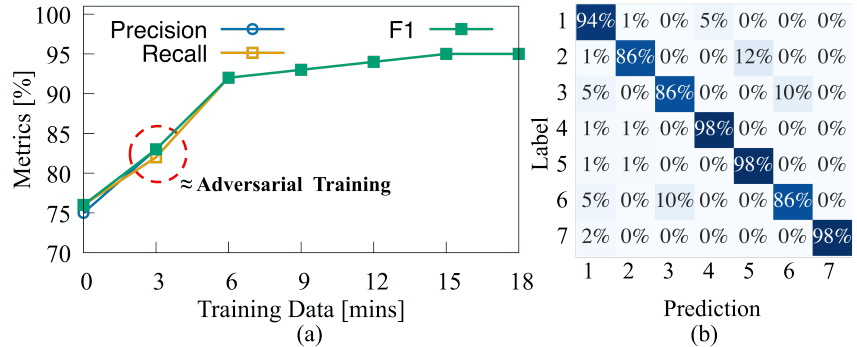


Fig. 14. Results of the personalized model, including (a) impact of training data volume on posture detection accuracy and (b) confusion matrix for posture detection: 1 Supine, 2 Left, 3 Right, 4 Hooking, 5 Left Fetal, 6 Right Fetal, 7 Prone.

dataset. Disabling the adversarial training module also led to a 7% decrease in classifying seven poses, reaffirming its role in enhancing cross-user generalization.

Furthermore, no significant impact was observed from factors such as neck circumference, hairstyle, or sweating on posture classification accuracy. Specifically, the six participants with nape hair achieved a comparable F1 score of 89% for seven-posture classification, relative to 88% for the fifteen participants without nape hair. This minor difference is partially attributed to the lower frequency of leg-bending postures within the group with nape hair.

Key Observations. The results from both studies highlight several key insights. PillowSense achieves consistently high accuracy in detecting upper-body postures across controlled and real-world settings, exhibiting only a modest performance degradation in natural conditions due to variations in sleep behavior. For detailed classification analysis, we present the confusion matrix from the lab study, as it features a balanced distribution of all postures. As shown in Fig. 12(b), most misclassifications occur when discriminating between similar upper-body postures paired with differing leg positions.

Furthermore, the posture change frequency observed in the longitudinal study indicates that healthy individuals tend to move infrequently during sleep. This behavior underscores the efficiency of leveraging movement detection triggers to conserve computational resources by activating posture classification algorithms only when necessary. We anticipate that individuals with sleep disorders may exhibit more frequent movements, and we plan to investigate these patterns in future clinical studies (§6). In addition, while leg bending detection remains effective, its slightly lower accuracy reflects both the limited availability of training data and the inherent challenges associated with inferring lower body movements from neck-based sensing.

Overall, while the lab study provided a balanced dataset ideal for comprehensive model validation, the longitudinal study emphasized PillowSense's robustness and practical applicability in everyday scenarios. At the same time, it revealed challenges related to user-specific factors such as hair density, sleep habits, and sensor contact stability. These findings highlight the potential benefits of incorporating adaptive calibration strategies to further improve system reliability in diverse real-world conditions, as discussed in §6.

5.2.2 Personalized Model. Since pillows are inherently personal, it is feasible to develop a personalized model for sleep monitoring. Given the variability in both the number of sleep postures and the duration of each posture across participants in the longitudinal study, we focus on the lab study to evaluate the personalized model for posture classification. While training this personalized model, we deactivate the user discriminator module. A critical consideration in personalized models is balancing training overhead and classification accuracy. We utilize varying portions of a participant's data for training and testing to evaluate this trade-off.

Table 2. Overall Vital Signs Estimation Results

Study	Group	HR [bpm]		RR [rpm]	
		Range	MAE	Range	MAE
Lab Study	Female	68–92	2.7	13–19	2.5
	Male	70–88	2.4	12–18	2.2
	Overall	68–92	2.5	12–19	2.4
Longitudinal Study	Female	55–86	2.6	13–18	2.9
	Male	48–91	2.7	11–19	3.2
	Overall	48–91	2.7	11–19	3.1

Table 3. Vital Sign Estimation by Participant Characteristics

	Group	HR MAE [bpm]	RR MAE [rpm]
Hair-style	Straight Short Hair (n=8)	2.5	2.9
	Curly Short Hair (n=3)	2.9	3.2
	Straight Long Hair (n=6)	2.6	3.0
	Curly Long Hair (n=4)	3.0	3.3
Nape Hair	Yes (n=6)	3.0	3.3
	No (n=15)	2.6	2.9
Sleep Sweating	Yes (n=3)	2.4	2.7
	No (n=18)	2.8	3.2

We randomly select an equal amount of data from each posture to compile the training set, while the remainder serves as the testing set. Since the same user performed multiple rounds of data collection in identical postures, this approach also influences the system's ability to handle subtle variations within the same posture for the same individual. The average data duration per participant is 51.7 minutes. The results depicted in Figure 14(a) lead to two key observations: (1) The generic model with adversarial training performs similarly to the personalized model when using approximately 3.5 minutes of training data (30 seconds per category), reaffirming the effectiveness of the user discriminator module. (2) With about 7 minutes of data (1 minute for each posture, equating to 15% of the total data per user), the overall classification performance is significantly improved, achieving precision, recall, and an F1 score of 92%. The confusion matrix shown in Figure 14(b) indicates a substantial error reduction particularly in leg bending. The largest source of error arises from the right and right-fetal positions, possibly because when sleepers sleep on their right side, the ECG signals are weaker with the heart being farthest from the sensors. Overall, these findings suggest that a personalized model, with just 7-minute training data, can substantially enhance posture classification accuracy.

5.3 Vital Sign Inference

After synchronizing the timestamps of our HR and RR estimates with the Pulse Oximeter ground truth data and the Apple Watch HR data, we identify a consistent time offset of approximately 2.1 and 5.2 seconds between our estimations and their measurements. This discrepancy is typical as commercial devices often report average HR and RR over a duration. Since the delay is unknown in advance, we compensate for this by applying a fixed delay adjustment, specific to each participant, to the inferred HR data.

Lab Study Results. As shown in Table 2, in the lab study, PillowSense estimates HR and RR with an MAE of 2.5 bpm and 2.4 rpm, respectively. Notably, there is a difference in the average MAE between males and females. We conduct two independent t-tests to explore the impact of gender on HR and RR estimation accuracy. We see no significant effect for gender on HR estimation, $t(20) = 2.62, p = 0.013$, although females exhibit slightly higher MAE values ($M = 2.71, SD = 1.03$) than males ($M = 2.39, SD = 1.21$). There is also no significant effect for gender on RR estimation, $t(20) = 2.312, p = 0.021$, despite females reporting slightly higher MAE values ($M = 2.51, SD = 0.51$) than males ($M = 2.24, SD = 0.21$).

Longitudinal Study Results. As outlined in the previous section, during the in-the-wild longitudinal study, a total of 912.2 hours of sleep data were recorded. Among this, 71.2 hours (approximately 7.8%) were identified as data loss due to intermittent loss of contact between the neck and the pillow sensors. These segments were excluded from subsequent analysis to ensure fair and accurate comparison. Detailed MAE for the estimation of HR and RR among all participants are presented in Table 2.

We observed no significant correlation between neck circumference and the accuracy of HR or RR estimation. Interestingly, participants reporting frequent sleep-related sweating showed improved estimation accuracy, with lower MAEs for HR (2.4 bpm vs. 2.8 bpm) and RR (2.7 rpm vs. 3.2 rpm), indicating enhanced signal quality. Welch's t-tests revealed statistically significant differences between the sweating and non-sweating groups, with $t(19) = 6.251, p < 0.001$ for HR and $t(19) = 7.814, p < 0.001$ for RR estimation. This finding suggests that slight moisture at the skin-sensor interface will enhance skin conductivity, benefiting biopotential acquisition.

Regarding hairstyle, participants with curly hair showed higher MAEs compared to those with straight hair (Table 3), reflecting a measurable reduction in estimation accuracy associated with curly hairstyles ($t(19) = -17.201, p < 0.001$ for HR estimation and $t(19) = -13.049, p < 0.001$ for RR estimation). Additionally, short-haired participants had marginally higher MAE values than those with long hair, though this difference was not statistically significant. Notably, participants with long hair were instructed to tie or reposition their hair prior to sleep, likely contributing to more stable sensor contact.

A clearer impact emerged from the presence of the nape hair, with participants with nape hair showing higher MAEs than those without nape hair (Table 3). Further analysis indicated all six participants with nape hair also had curly hairstyles, suggesting that reduced accuracy associated with curly hair primarily stems from nape hair interference, disrupting consistent sensor contact ($t(19) = -15.442, p < 0.001$ for HR estimation and $t(19) = -14.250, p < 0.001$ for RR estimation).

Finally, when comparing HR estimations between our system and the Apple Watch (treated as the reference), our system demonstrated an overall MAE of 2.1 bpm, lower than the MAE observed using the pulse oximeter as ground truth. This result indicates that our system achieves comparable accuracy in vital sign monitoring when compared to consumer wearable devices.

Key Observations. The evaluation of PillowSense across both controlled (lab) and real-world (longitudinal) settings provides several important insights into its capability for vital sign monitoring during sleep.

First, in both studies, PillowSense demonstrated reliable HR and RR estimation, with MAE values comparable to FDA-approved clinical devices [1, 73]. Notably, in both settings, gender showed no significant impact on estimation accuracy, although females exhibited slightly higher MAE values, likely due to generally lower ECG voltage amplitudes—a trend aligned with existing literature [81, 84, 108]. In the meantime, one key limitation of the current prototype is its inability to consistently maintain optimal sensor-neck contact, which compromises the reliability of vital signs monitoring.

Second, while performance in the longitudinal study was slightly lower than in the lab setting – reflecting the challenges posed by natural variability, user movement, and occasional sensor contact loss – it remained within acceptable clinical thresholds (i.e., within the 3 bpm error standard for HR).

Third, the longitudinal study further revealed the influence of user-specific factors not observable in controlled environments. In particular, frequent sleep-related sweating was associated with improved estimation accuracy, likely due to enhanced skin-sensor conductivity. Conversely, participants with curly hair, and especially those with nape hair, experienced significantly higher MAE values, highlighting the impact of hair texture and placement on sensor performance. The difference between short and long hair was minimal and not statistically significant, possibly mitigated by instructions for participants with long hair to secure their hair before sleep.

These findings collectively emphasize both the strengths and areas for potential improvement of PillowSense, reinforcing its viability as a comfortable, non-intrusive sleep monitoring solution for daily application. Addressing identified factors such as sensor-contact stability and hair interference through improved design or adaptive calibration strategies will further enhance system robustness and usability.

5.4 Usability

Comfort and usability are critical for the long-term adoption of sleep monitoring systems, particularly when embedded into everyday objects like pillows. We collected user feedback from both the lab study ($N = 20$) and the longitudinal study ($N = 21$) through a standardized questionnaire and open-ended comments. The questionnaire employs a standard 5-point Likert scale for responses, ranging from (1) Strongly Disagree, (2) Disagree, (3) Neutral, (4) Agree, and (5) Strongly Agree, covering the following aspects:

- Q1: The pillow is very comfortable in terms of touching experience.
- Q2: The touching feeling of the pillow is almost the same as a normal pillow at home.
- Q3: The comfort level of the pillow's sensing fabric is better compared to typical sleep monitoring devices (e.g., Apple Watch, sleep eye mask, sleep belt).
- Q4: I am likely to use a sleep monitoring system.
- Q5: If I wanted to monitor my sleep daily, I would prefer the pillow prototype over current commercial sleep monitoring devices (e.g., Apple Watch, sleep eye mask, sleep belt).

As shown in Figure 15, participants across both studies rated the PillowSense pillow prototype positively in terms of comfort, with average scores of 4.0 (lab) and 4.1 (longitudinal) for overall tactile experience (Q1). Interestingly, while comfort perception was slightly improved with prolonged use, participants in the longitudinal study rated the similarity to their home pillow (Q2) marginally lower (3.5) compared to the lab study (3.7). This suggests that, over extended use, subtle differences from personal pillows became more noticeable.

A consistent observation across both studies is the strong preference for PillowSense over wearable-based sleep monitoring devices. Participants rated the comfort of the sensing fabric higher in the longitudinal study (4.6) than in the lab (4.4) for Q3, indicating that real-world use reinforced the advantage of passive, non-intrusive monitoring. Similarly, preference for using the pillow system over conventional devices (Q5) remained high, with scores of 4.1 and 4.2 in the lab and longitudinal studies.

Willingness to adopt sleep monitoring (Q4) remained moderate in both settings (3.2 in lab, 3.3 in longitudinal), with participants frequently citing privacy concerns regarding data sharing as a primary hesitation. Additionally, several participants emphasized the desire for enhanced functionalities, such as sleep stage tracking and snore detection, to increase daily usage motivation.

Overall, these findings indicate that PillowSense's design offers reasonable comfort and user acceptance compared to traditional wearables, particularly during extended real-world use. Addressing privacy concerns and expanding system features will be key to improving long-term adoption and user engagement.

5.5 Practical Considerations

Multi-User Scenario. Considering the common occurrence of multiple users sharing a bed, we conducted a separate study with two pairs of participants (1 male and 3 female). We instruct one participant to assume various postures on PillowSense while the other shares the same bed. The second user participates in typical bedtime activities, simulating a normal home environment. We collect data for 2 hours from each pair. Overall, PillowSense achieves an average F1 score of 98.2% in distinguishing between left, right, supine, and prone postures. The classification accuracy for seven postures is 85% with the generic model and 93% with the personalized model.

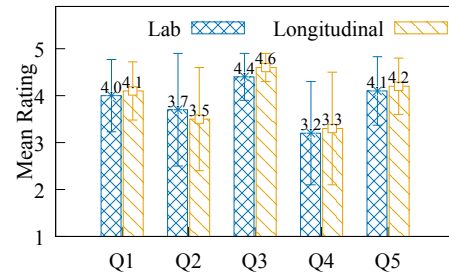


Fig. 15. Participant ratings in both the lab and longitudinal studies.

The average MAE for HR and RR measurements is 2.7 bpm and 2.5 rpm, respectively. These results are comparable to those observed in single-user scenarios, indicating PillowSense’s robustness in managing multiple users.

Washing/Cleaning. To evaluate the prototype’s washability, We detach the fabric sensor array from the rest of the pillowcase and explore two cleaning methods: wiping with sanitizing wipes and hand washing, followed by air drying². We confirm with doctors that using sanitizing wipes is an acceptable cleaning practice in clinical settings. For this study, we fabricate three prototypes of the biopotential sensing layer, where one is cleaned with sanitizing wipes 50 times, one is hand washed 5 times, and the third serves as the control, undergoing no cleaning. After each cleaning cycle, we record the ECG signals of a participant (a 28-year-old male) for ten minutes using the cleaned prototype and the control prototype simultaneously. A direct comparison for sEMG is challenging because sensing electrodes cannot be consistently placed at identical locations, resulting in variability in sEMG signals due to differences in sensor positioning. Since sEMG and ECG share the same sensing circuit, the ECG results indicate what to expect with sEMG.

To assess the impact of each cleaning method on the integrity of the ECG signals, we compare the HR computed from the ECG data of the cleaned layers with those from the control group. Additionally, we calculate the Pearson correlation coefficient (PCC) between these data. As shown in Figure 16, all of the PCC scores are higher than 0.95. For the prototype cleaned with sanitizing wipes, the average estimated HR differences after 10, 20, 30, 40, and 50 cycles are 0.1, 0.2, 0.1, 0.1, and 0.2 bpm, respectively. For the hand-washed prototype, the average estimated HR differences after 1, 2, and 3 cycles were 0.2, 0.1, and 0.1 bpm, respectively. These findings suggest that both cleaning methods entail minimal impact on the integrity of the ECG signal.

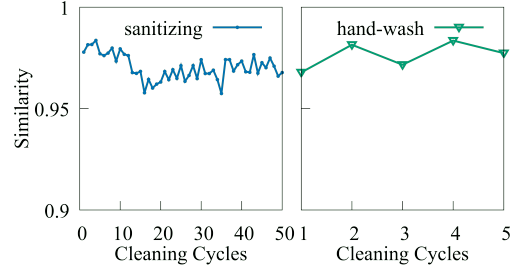


Fig. 16. ECG similarity score before and after cleaning.

Power Consumption. We evaluate system power consumption using a power monitor [25]. Since the algorithms for sleep variable inference currently run offline (we will discuss implementation optimization in §6), the power evaluation focuses on sensing data collection. This involves two microcontrollers (MCUs) and the sensor array. The OpenBCI board, responsible for biopotential data collection, consumes 170.2 mW at 3.6 V. The Arduino Due board, along with multiplexers managing channel selection, consumes 392.2 mW at 3.3 V. The integration of the pressure sensor array allows the biopotential sensor array to use one 8-channel analog-to-digital converter (ADC) at 41 mW for 6 channels of data, saving 287 mW (i.e., achieving 50% power reduction) compared to using 8 ADCs for 60 channels. Theoretically, the architecture does not necessitate two separate MCUs. Future developments can further reduce power consumption by integrating all processing into a single MCU.

6 DISCUSSIONS AND FUTURE WORK

Hair Blockage. Hair blockage remains a challenge for the current design. In the study we instructed users with longer hair to tie their hair back or move it aside. While this practice is adopted by individuals with long hair during sleep and entails minimal operational overhead, we seek to better handle hair in future work. Capacitive sensing is a potential alternative, given its ability to detect biopotential signals through insulating materials such as clothing without requiring direct contact with human skin [79, 80, 94]. Although our initial attempts to implement a similar circuit did not yield signals with sufficiently robust SNR, we were able to detect biopotential signals with low-impedance insulating layers (e.g., wet clothes). Further research can optimize circuit design to improve signal SNR in other conditions.

²We do not include machine washing because the flexible PCBs in the prototype cannot be detached and they are not machine washable.

Clinical Study. We are working with our medical collaborator to prepare for a clinical study in sleep laboratories involving patients with sleep issues. It will provide a larger and more diverse dataset to potentially improve the performance of our neural network module, which typically requires large datasets for optimal training. It will allow us to more comprehensively assess the clinical usability of PillowSense for patients.

Sleep Staging. With inference results of sleep poses, vital signs, and body movement, a potential next step is to study the feasibility of fusing these sleep variables to determine sleep stages such as light sleep, deep sleep, and rapid eye movement sleep. Movement data can indicate shifts between lighter and deeper sleep stages, while HR and RR fluctuations provide insights into the autonomic nervous system's activity during different sleep phases [94]. Technologies such as the Apple Watch utilize a similar set of data for sleep staging, yielding promising results [5, 115]. Feedback from our users indicates a preference for non-rigid wearables during sleep. Thus, sleep staging using only a pillow is a valuable future research direction.

Decoupling ECG and sEMG. Our current system relies on traditional bandpass filtering to isolate dominant frequency components of ECG and sEMG based on low-amplitude, noise-prone biopotential signals collected from the neck. This method, however, does not achieve true signal separation and offers limited interpretability. A more principled approach (e.g., blind source separation, or model-driven signal decomposition) can enhance signal fidelity and improve generalizability. It can also enable rule-based classification schemes, which will reduce reliance on neural networks and increase the transparency and clinical interpretability of sleep variable inference.

Prototype Refinement. A future prototype refinement is to seek optimized pillow shapes to improve the neck-to-skin contact. For instance, a U-shaped pillow cradles the head in a fixed position, significantly reducing the likelihood of the head moving off the pillow during sleep. Furthermore, enhanced isolation between the electrodes is crucial to prevent cross-connection caused by excessive moisture (e.g., saliva), which could occur during sleep. We will also optimize the processing pipeline and explore on-device neural network inference to realize real-time inference of sleep variables. Additionally, we can seek a more adaptable connection method between conductive threads and flexible PCBs so that the latter can be detached to allow the prototype to be machine washable. These advancements can transition the research prototype to a practical monitoring tool.

7 RELATED WORK

Sleep Posture Monitoring. We divide the existing work on sleep posture monitoring into two main categories:

(1) *Wearable*: Wearable sensors are prevalently utilized for sleep monitoring, as documented in several studies [13, 14, 47, 48, 98, 122]. Jeon et al. developed a sleep position tracking system that includes two wristbands and a chest band, all incorporating Inertial Measurement Unit (IMU) data [48]. Wristbands are particularly favored for sleep posture monitoring due to their ease of use and non-intrusive nature [14, 47]. Rofouei et al. introduced an innovative approach using a neck cuff equipped with pulse oximeters, microphones, and an accelerometer [98]. However, all these wearable solutions still require users to wear extra components, which can diminish comfort during sleep. Our approach aims to monitor sleep postures and vital signs without altering the user's natural sleeping experience, addressing the comfort limitations associated with wearable technologies.

(2) *Infrastructure-based*: The trend toward infrastructure-based sleep monitoring solutions has grown due to their non-intrusive nature [6, 33, 36, 37, 63, 66, 68, 69, 83, 92, 119, 124]. These methods leverage various technologies, such as pressure-sensitive bed sheets [65], radio frequency signals [95, 123, 124], and camera-based monitoring [23]. In comparison, PillowSense presents lower instrumentation overhead and is less susceptible to ambient interference. By embedding sensing fabrics into individual pillowcases, PillowSense handles multi-user scenarios more effectively. Furthermore, PillowSense senses multiple sleep variables concurrently.

Vital Sign Monitoring. Many commercial wearable devices like the Apple Watch S6, use photoplethysmography to measure heart rates. Additionally, [102] presents the use of pressure-sensitive microbend fiber optic sensors

attached to the user's back to infer heart rate and respiration rate. Phyjama [53] and PhyMask [99] are innovative wearable systems that utilize fabric sensors for vital sign monitoring. However, they still require users to wear special items. Focusing on vital signs, they offer limited capabilities in posture classification. Active research also studies non-contact vital sign monitoring using acoustic signals [15, 78] and radio frequency signals such as Wi-Fi [64, 124] and mmWave [121]. These methods are prone to ambient interference and face significant challenges in dealing with multiple users and surrounding moving objects.

Smart Pillow Sensing. Existing research on smart pillows [3, 56, 59, 113] explores various solutions for sleep quality monitoring. However, many of these approaches rely on rigid sensors embedded in pillows or require additional wearable devices, potentially disrupting the user's sleep experience and limiting their practicality in daily use. Kou et al. [56] developed a triboelectric nanogenerator (FB-TENG) sensor array that tracks head movement by detecting pressure changes with a self-powered pressure sensor. While promising, this approach cannot monitor lower-body movements or vital signs. An IoT-based smart pillow [113] integrates temperature, humidity, sound, and vibration sensors on the pillow's surface to assess sleep quality; however, the rigidity of these sensors makes them uncomfortable for practical use. Similarly, Ali et al. [3] implemented a smart pillow system for detecting and managing sleep apnea using pulse oximeters and accelerometers, which can adjust the pillow's position and issue alarms during severe apnea events. Although this approach offers valuable intervention capabilities, it still requires users to wear additional sensors, reducing convenience.

Fabric-based Biopotential Sensing. Prior works have studied various textile sensors [27, 29, 67, 87, 104, 106]. Polymer-based textile electrodes, created by printing conductive paste onto cotton fabrics, sense sEMG signals effectively when an electrolyte is applied, though their performance degrades under dry conditions due to increased noise [87]. Electrodes made from conductive yarns blending silver fibers with non-conductive synthetic materials require moisturization to maintain performance, akin to conventional gel electrodes [29]. Additionally, textile electrodes made from stainless steel fibers integrated into a non-conductive nylon and elastane matrix are used in stroke rehabilitation to monitor muscle activities [27]. PillowSense differs in utilizing fabric sensors made of off-the-shelf conductive fabrics and enhancing their sensing performance with computational methods.

8 CONCLUSION

We designed, implemented, and evaluated PillowSense, which integrates soft fabric sensors into everyday pillowcases. Utilizing ECG and sEMG signals from the neck, PillowSense effectively monitors sleep postures, vital signs, and body movement. Prototype testing with 21 participants demonstrated its accuracy in sleep posture estimation with an average F1-score of 88%, and vital sign inference with clinically acceptable accuracy. PillowSense offers promising potential for non-intrusive, large-scale sleep monitoring without disrupting normal sleep routines.

Acknowledgments

We sincerely thank our reviewers for their insightful feedback. We thank Dr. Hardy J. Schwartz for the clinical ECG consultation. This work was supported in part by the National Science Foundation (IIS 2202553), the Columbia Research Initiatives in Science & Engineering (RISE) Award, and The Hong Kong Center for Construction Robotics (InnoHK-HKCRC), an InnoHK center supported by the Hong Kong Innovation and Technology Commission (ITC). Any opinions, findings, conclusions, or recommendations expressed in this material are those of the authors and do not necessarily reflect those of the funding agencies or others.

References

- [1] 2020. *masimoFDA*. Retrieved Jun 1, 2024 from https://www.accessdata.fda.gov/cdrh_docs/pdf19/K193242.pdf

- [2] Raul Alcaraz and José Joaquín Rieta. 2010. EMD-based filtering for baseline wander and powerline interference cancellation in ECG signals. *Computers in Biology and Medicine* 40, 11-12 (2010), 931–938.
- [3] Syeda Zuriat-e-Zehra Ali, Rida Ashfaq, Rameesa Afzal, Mehr-UN-Nisa, Babar Sultan, and Abdul Jalil. 2019. Smart Pillow:Sleep Apnea Monitoring and Minimization Device. In *2019 7th International Conference on Robot Intelligence Technology and Applications (RiTA)*. 215–219. <https://doi.org/10.1109/RITAPP.2019.8932822>
- [4] Janome America. 2015. *Janome America: World's Easiest Sewing, Quilting, Embroidery Machines - Memory Craft 500E*. Retrieved June 23, 2024 from <https://www.janome.com/machines/embroidery/memory-craft-500e>
- [5] Apple. 2023. *Estimating Sleep Stages from Apple Watch*. Retrieved June 1, 2024 from https://www.apple.com/healthcare/docs/site/Estimating_Sleep_Stages_from_Apple_Watch_Sept_2023.pdf
- [6] Paolo Baroscchi. 2012. Position recognition to support bedsores prevention. *IEEE journal of biomedical and health informatics* 17, 1 (2012), 53–59. <https://doi.org/10.1109/TIB.2012.2220374>
- [7] Gary G Berntson, John T Cacioppo, and Karen S Quigley. 1993. Respiratory sinus arrhythmia: Autonomic origins, physiological mechanisms, and psychophysiological implications. *Psychophysiology* 30, 2 (1993), 183–196.
- [8] William Boissonnault and Richard P. Di Fabio. 1996. Pain Profiles of Patients With Low Back Pain Referred to Physical Therapy. *Journal of Orthopaedic & Sports Physical Therapy* 24, 4 (1996), 180–91. <https://doi.org/10.2519/jospt.1996.24.4.180>
- [9] Rohit Budhiraja, Tauseef A. Siddiqi, and Stuart F. Quan. 2015. Sleep Disorders in Chronic Obstructive Pulmonary Disease: Etiology, Impact, and Management. *Journal of Clinical Sleep Medicine* 11, 03 (2015), 259–70. <https://doi.org/10.5664/jcsm.4540>
- [10] Daniel J Buysse, Ron Grunstein, Jim Horne, and Peretz Lavie. 2010. Can an improvement in sleep positively impact on health? *Sleep medicine reviews* 14, 6 (2010), 405–410.
- [11] Mary A Carskadon, William C Dement, et al. 2005. Normal human sleep: an overview. *Principles and practice of sleep medicine* 4, 1 (2005), 13–23.
- [12] Doug Cary, Angela Jacques, and Kathy Briffa. 2021. Examining relationships between sleep posture, waking spinal symptoms and quality of sleep: A cross sectional study. *PLOS ONE* 16, 11 (2021), e0260582. <https://doi.org/10.1371/journal.pone.0260582>
- [13] Kang-Ming Chang and Shin-Hong Liu. 2011. Wireless portable electrocardiogram and a tri-axis accelerometer implementation and application on sleep activity monitoring. *Telemedicine and e-Health* 17, 3 (2011), 177–184. <https://doi.org/10.1089/tmj.2010.0078>
- [14] Liqiong Chang, Jiaqi Lu, Ju Wang, Xiaojiang Chen, Dingyi Fang, Zhanyong Tang, Petteri Nurmi, and Zheng Wang. 2018. SleepGuard: Capturing rich sleep information using smartwatch sensing data. *Proceedings of the ACM on Interactive, Mobile, Wearable and Ubiquitous Technologies* 2, 3 (2018), 1–34.
- [15] Xiangmao Chang, Cheng Peng, Guoliang Xing, Tian Hao, and Gang Zhou. 2020. Isleep: A smartphone system for unobtrusive sleep quality monitoring. *ACM Transactions on Sensor Networks (TOSN)* 16, 3 (2020), 1–32.
- [16] Sudhansu Chokroverty. 2010. Overview of sleep & sleep disorders. *Indian Journal of Medical Research* 131, 2 (2010), 126–140.
- [17] François Fleuret. 2017. Kception: Deep Learning with Depthwise Separable Convolutions. In *2017 IEEE Conference on Computer Vision and Pattern Recognition (CVPR)*. 1800–1807. <https://doi.org/10.1109/CVPR.2017.195>
- [18] Florian Chouchou and Martin Desseilles. 2014. Heart rate variability: a tool to explore the sleeping brain? *Frontiers in neuroscience* 8 (2014), 116837.
- [19] Gih Sung Chung, Byoung Hoon Choi, Ko Keun Kim, Yong Gyu Lim, Jin Wook Choi, Do-Un Jeong, and Kwang Suk Park. 2007. REM Sleep Classification with Respiration Rates. *2007 6th International Special Topic Conference on Information Technology Applications in Biomedicine* (2007), 194–97. <https://doi.org/10.1109/ITAB.2007.4407379>
- [20] Cricut. 2024. *Cricut*. Retrieved June 25, 2024 from <https://cricut.com/en-us/cutting-machines/cricut-maker/cricut-maker-3/cricut-maker-3/2008334.html>
- [21] Mission Darkness. 2024. *Mission Darkness TitanRF Faraday Tape // 1in W x 10ft L (2.54cm x 3.05m) High-Shielding Conductive Adhesive Tape Roll Used to Connect TitanRF Fabric Sheets or Seal RF Enclosures*. Retrieved June 25, 2024 from https://www.amazon.com/dp/B07CRLCGCHstarsLeft=1&ref_=cm_sw_r_cso_cp_apin_dp_TD3RGZH1PECJF1HG4C7A&th=1
- [22] Joseph De Koninck, Dominique Lorrain, and Pierre Gagnon. 1992. Sleep positions and position shifts in five age groups: an ontogenetic picture. *Sleep* 15, 2 (1992), 143–149.
- [23] Fei Deng, Jianwu Dong, Xiangyu Wang, Ying Fang, Yu Liu, Zhaofei Yu, Jing Liu, and Feng Chen. 2018. Design and implementation of a noncontact sleep monitoring system using infrared cameras and motion sensor. *IEEE Transactions on Instrumentation and Measurement* 67, 7 (2018), 1555–1563.
- [24] Analog Devices. 2025. *MAX14661*. Retrieved April 27, 2025 from <https://www.analog.com/en/products/max14661.html>
- [25] eBay. 2023. *Monsoon Solutions FTA22D Power Monitor*. Retrieved June 1, 2024 from https://www.ebay.com/item/264423084756?mkcid=16&mkevt=1&mkruid=711-127632-2357-0&sssp=mnMh23DaTOe&ssrc=2047675&ssuid=&widget_ver=artemis&media=COPY
- [26] ECGwaves. 2023. *ECG&Echo Learning*. Retrieved June 15, 2023 from <https://ecgwaves.com/course/the-ecg-book/>
- [27] Lorussi Federico, Carbonaro Nicola, De Rossi Danilo, Paradiso Rita, Veltink Peter, and Tognetti Alessandro. 2016. Wearable Textile Platform for Assessing Stroke Patient Treatment in Daily Life Conditions. *Frontiers in Bioengineering and Biotechnology* 4 (2016). <https://doi.org/10.3389/fbioe.2016.00028>

- [28] Gabriela Figas, Anna Hadamus, Michalina Błażkiewicz, and Jolanta Kujawa. 2023. Symmetry of the Neck Muscles' Activity in the Electromyography Signal during Basic Motion Patterns. *Sensors* 23, 8 (2023), 4170.
- [29] T Finni, M Hu, P Kettunen, T Vilavuo, and S Cheng. 2007. Measurement of EMG activity with textile electrodes embedded into clothing. *Physiological Measurement* 28, 11 (2007), 1405. <https://doi.org/10.1088/0967-3334/28/11/007>
- [30] Yaroslav Ganin, Evgeniya Ustinova, Hana Ajakan, Pascal Germain, Hugo Larochelle, François Laviolette, Mario Marchand, and Victor Lempitsky. 2016. Domain-Adversarial Training of Neural Networks. 17, 1 (Jan. 2016), 2096–2030.
- [31] Physix Gear. 2024. *Physix Gear Sport Kinesiology Tape (2 Pack or 1 Pack), Best Waterproof Muscle Support Adhesive, 2in x 16.4ft Roll Uncut, Physio Therapeutic Aid for Injury Recovery*. Retrieved June 25, 2024 from https://www.amazon.com/dp/B012G0YSMW?m=AFMT9MT9F4PJ&ref=psp_pc_a_A148PVPKBOG2NI&th=1
- [32] Ruth Gilbert, Georgia Salanti, Melissa Harden, and Sarah See. 2005. Infant sleeping position and the sudden infant death syndrome: systematic review of observational studies and historical review of recommendations from 1940 to 2002. *International Journal of Epidemiology* 34, 4 (2005), 874–887. <https://doi.org/10.1093/ije/dyi088>
- [33] Timo Grimm, Manuel Martinez, Andreas Benz, and Rainer Stiefelhagen. 2016. Sleep position classification from a depth camera using bed aligned maps. In *2016 23rd International Conference on Pattern Recognition (ICPR)*. IEEE, 319–324. <https://doi.org/10.1109/ICPR.2016.7899653>
- [34] Ta-Wei Guu, Marijn Muurling, Zunera Khan, Chris Kalafatis, Dag Aarsland, Anna-Katharine Brem, et al. 2023. Wearable devices: underrepresentation in the ageing society. *The Lancet Digital Health* 5, 6 (2023), e336–e337.
- [35] Feiyu Han, Panlong Yang, Yuanhao Feng, Weiwei Jiang, Youwei Zhang, and Xiang-Yang Li. 2024. EarSleep: In-ear Acoustic-based Physical and Physiological Activity Recognition for Sleep Stage Detection. *Proc. ACM Interact. Mob. Wearable Ubiquitous Technol.* 8, 2, Article 43 (May 2024), 31 pages. <https://doi.org/10.1145/3659595>
- [36] Enamul Hoque, Robert F Dickerson, and John A Stankovi. 2010. Monitoring body positions and movements during sleep using wisps. In *Wireless Health 2010*. ACM, 44–53. <https://doi.org/10.1145/1921081.1921088>
- [37] Chi-Chun Hsia, Yu-Wei Hung, Yu-Hsien Chiu, and Chia-Hao Kang. 2008. Bayesian classification for bed posture detection based on kurtosis and skewness estimation. In *HealthCom 2008-10th International Conference on e-health Networking, Applications and Services*. IEEE, 165–168. <https://doi.org/10.1109/HEALTH.2008.4600129>
- [38] Xiaoxuan Hu, Kagome Naya, Peng Li, Toshiaki Miyazaki, Kun Wang, and Yanfei Sun. 2018. Non-invasive sleeping posture recognition and body movement detection based on RFID. In *2018 IEEE International Conference on Internet of Things and IEEE Green Computing and Communications and IEEE Cyber, Physical and Social Computing and IEEE Smart Data*. IEEE, 1817–1820.
- [39] François Hug and Kylie Tucker. 2018. Surface electromyography to study muscle coordination. (2018).
- [40] Earable Inc. 2024. *FRENZ Brainband*. Retrieved June 1, 2024 from <https://frenzband.com/>
- [41] Ink/Stitch. 2023. *Ink/Stitch*. Retrieved June 25, 2024 from <https://inkstitch.org/>
- [42] Texas Instruments. 2024. *CD74HC4067*. Retrieved June 1, 2024 from <https://www.ti.com/lit/ds/symlink/xcd74hc4067.pdf>
- [43] Ali Isin and Selen Ozdalili. 2017. Cardiac arrhythmia detection using deep learning. *Procedia computer science* 120 (2017), 268–275.
- [44] Dressle Raphael J. and Dieter Riemann. 2023. Hyperarousal in Insomnia Disorder: Current Evidence and Potential Mechanisms. *Journal of Sleep Research* 32, 6 (2023), e13928. <https://doi.org/10.1111/jsr.13928>
- [45] Vaingankar JA, Müller-Riemenschneider F, Chu AHY, Subramaniam M, Tan LWL, Chong SA, and van Dam RM. 2022. Sleep Duration, Sleep Quality and Physical Activity, but Not Sedentary Behaviour, Are Associated with Positive Mental Health in a Multi-Ethnic Asian Population: A Cross-Sectional Evaluation. *International Journal of Environmental Research and Public Health* 17, 22 (2022), 8489.
- [46] Shahrokh Javaheri and M Safwan Badr. 2023. Central sleep apnea: pathophysiologic classification. *Sleep* 46, 3 (2023), zsac113.
- [47] Po-Yuan Jeng, Li-Chun Wang, Chaur-Jong Hu, and Dean Wu. 2021. A wrist sensor sleep posture monitoring system: An automatic labeling approach. *Sensors* 21, 1 (2021), 258.
- [48] Sanghoon Jeon, Taejoon Park, Anand Paul, Yang-Soo Lee, and Sang Hyuk Son. 2019. A Wearable Sleep Position Tracking System Based on Dynamic State Transition Framework. *IEEE Access* 7 (2019), 135742–135756. <https://doi.org/10.1109/ACCESS.2019.2942608>
- [49] Sharon MB Joines, Carolyn M Sommerich, Gary A Mirka, James R Wilson, and Samuel D Moon. 2006. Low-level exertions of the neck musculature: a study of research methods. *Journal of Electromyography and Kinesiology* 16, 5 (2006), 485–497.
- [50] Simon A. Joosten, Denise M. O'Driscoll, Philip J. Berger, and Garun S. Hamilto. 2014. Supine Position Related Obstructive Sleep Apnea in Adults: Pathogenesis and Treatment. *Sleep Medicine Reviews* 18, 1 (2014), 7–17. <https://doi.org/10.1016/j.smrv.2013.01.005>
- [51] Vimal Kakaraparthi, Qijia Shao, Charles J. Carver, Tien Pham, Nam Bui, Phuc Nguyen, Xia Zhou, and Tam Vu. 2021. FaceSense: Sensing Face Touch with an Ear-worn System. *Proc. ACM Interact. Mob. Wearable Ubiquitous Technol.* 5, 3, Article 110 (Sept. 2021), 27 pages. <https://doi.org/10.1145/3478129>
- [52] Walter Karlen, Srinivas Raman, J Mark Ansermino, and Guy A Dumont. 2013. Multiparameter respiratory rate estimation from the photoplethysmogram. *IEEE Transactions on Biomedical Engineering* 60, 7 (2013), 1946–1953.
- [53] Ali Kiaghadi, Seyedeh Zohreh Homayounfar, Jeremy Gummesson, Trisha Andrew, and Deepak Ganesan. 2019. Phyjama: Physiological sensing via fiber-enhanced pyjamas. *Proceedings of the ACM on Interactive, Mobile, Wearable and Ubiquitous Technologies* 3, 3 (2019), 1–29.

- [54] Joseph De Koninck, Pierre Gagnon, and Serge Lallier. 1983. Sleep Positions in the Young Adult and Their Relationship with the Subjective Quality of Sleep. *Sleep* 6, 1 (1983), 52–59. <https://doi.org/10.1093/sleep/6.1.52>
- [55] Peter Konrad. 2005. The abc of emg. *A practical introduction to kinesiological electromyography* 1, 2005 (2005), 30–5.
- [56] Haiying Kou, Haiming Wang, Renwei Cheng, Yanjun Liao, Xue Shi, Jianjun Luo, Ding Li, and Zhong Lin Wang. 2022. Smart Pillow Based on Flexible and Breathable Triboelectric Nanogenerator Arrays for Head Movement Monitoring during Sleep. *ACS Applied Materials and Interfaces* 14, 20 (2022), 23998–24007. <https://doi.org/10.1021/acsami.2c03056>
- [57] Vernon J Lawhern, Amelia J Solon, Nicholas R Waytowich, Stephen M Gordon, Chou P Hung, and Brent J Lance. 2018. EEGNet: a compact convolutional neural network for EEG-based brain-computer interfaces. *Journal of Neural Engineering* 15, 5 (jul 2018), 056013.
- [58] Won-Hwee Lee and Min-Seok Ko. 2017. Effect of sleep posture on neck muscle activity. *Journal of physical therapy science* 29, 6 (2017), 1021–1024.
- [59] Jason K. Liao, Chun Yin Lai, Chetwyn Che Hin Chan, and Steve W. Y. Mung. 2024. Design and Implementation of an IoT Acoustic-Controlled Pillow for Sleep Health Monitoring. *IEEE Sensors Letters* 8, 9 (2024), 1–4. <https://doi.org/10.1109/LSENS.2024.3439259>
- [60] Compumedics Limited. 2024. *Somfit*. Retrieved June 1, 2024 from <https://www.compumedics.com.au/en/products/somfit>
- [61] Chen Liu, Zixuan Dong, Li Huang, Wenlong Yan, Xin Wang, Dingyi Fang, and Xiaojiang Chen. 2024. TagSleep3D: RF-based 3D Sleep Posture Skeleton Recognition. 8, 1, Article 13 (March 2024), 28 pages. <https://doi.org/10.1145/3643512>
- [62] Jia Liu, Xingyu Chen, Shigang Chen, Xiulong Liu, Yanyan Wang, and Lijun Chen. 2019. TagSheet: Sleeping posture recognition with an unobtrusive passive tag matrix. In *IEEE INFOCOM 2019-IEEE Conference on Computer Communications*. IEEE, 874–882.
- [63] Jian Liu, Yingying Chen, Yan Wang, Xu Chen, Jerry Cheng, and Jie Yang. 2018. Monitoring vital signs and postures during sleep using WiFi signals. *IEEE Internet of Things Journal* 5, 3 (2018), 2071–2084. <https://doi.org/10.1109/JIOT.2018.2822818>
- [64] Jian Liu, Yan Wang, Yingying Chen, Jie Yang, Xu Chen, and Jerry Cheng. 2015. Tracking Vital Signs During Sleep Leveraging Off-the-Shelf WiFi. In *Proceedings of the 16th ACM International Symposium on Mobile Ad Hoc Networking and Computing*. ACM Digital Library, 267–276. <https://doi.org/10.1145/2746285.2746303>
- [65] Jason J Liu, Wenyao Xu, Ming-Chun Huang, Nabil Alshurafa, Majid Sarrafzadeh, Nitin Raut, and Behrooz Yadegar. 2013. A dense pressure sensitive bedsheet design for unobtrusive sleep posture monitoring. In *2013 IEEE international conference on pervasive computing and communications (PerCom)*. IEEE, 207–215.
- [66] Jason J Liu, Wenyao Xu, Ming-Chun Huang, Nabil Alshurafa, Majid Sarrafzadeh, Nitin Raut, and Behrooz Yadegar. 2014. Sleep posture analysis using a dense pressure sensitive bedsheet. *Pervasive and Mobile Computing* 10 (2014), 34–50.
- [67] Ruibo Liu, Qijia Shao, Siqi Wang, Christina Ru, Devin Balkcom, and Xia Zhou. 2019. Reconstructing Human Joint Motion with Computational Fabrics. *Proc. ACM Interact. Mob. Wearable Ubiquitous Technol.* 3, 1, Article 19 (March 2019), 26 pages. <https://doi.org/10.1145/3314406>
- [68] Shuangjun Liu and Sarah Ostadabbas. 2017. A vision-based system for in-bed posture tracking. In *2017 IEEE International Conference on Computer Vision Workshops (ICCVW)*, 1373–1382. <https://doi.org/10.1109/ICCVW.2017.163>
- [69] Xuefeng Liu, Jiannong Cao, Shaojie Tang, and Jiaqi Wen. 2014. Wi-Sleep: Contactless sleep monitoring via WiFi signals. In *2014 IEEE Real-Time Systems Symposium*. IEEE, 346–355. <https://doi.org/10.1109/RTSS.2014.30>
- [70] Donald M. Lloyd-Jones, Norrina B. Allen, Cheryl A.M. Anderson, Terrie Black, LaPrincess C. Brewer, Randi E. Foraker, Michael A. Grandner, Helen Lavretsky, Amanda Marma Perak, Garima Sharma, Wayne Rosamond, and on behalf of the American Heart Association. 2022. Life's Essential 8: Updating and Enhancing the American Heart Association's Construct of Cardiovascular Health: A Presidential Advisory From the American Heart Association. *Circulation* 146, 5 (2022), e18–e43.
- [71] Geraldo Lorenzi-Filho, Pedro R Genta, Adelaide C. Figueiredo, and Daniel Inoue. 2005. Cheyne-stokes respiration in patients with congestive heart failure: causes and consequences. *Clinics* 60, 4 (2005), 333–44. <https://doi.org/10.1590/S1807-59322005000400012>
- [72] Masimo. 2019. *MightySat™ Rx Fingertip Pulse Oximeter*. Retrieved March 21, 2024 from https://techdocs.masimo.com/globalassets/techdocs/pdf/lab-10169a_master.pdf
- [73] Masimo. 2024. *MightySat Medical*. Retrieved June 25, 2024 from <https://www.masimo.com/en-us/product/health-monitoring/137737.html>
- [74] Lara McManus, Giuseppe De Vito, and Madeleine M Lowery. 2020. Analysis and biophysics of surface EMG for physiotherapists and kinesiologists: Toward a common language with rehabilitation engineers. *Frontiers in neurology* 11 (2020), 576729.
- [75] Akshay Menon and Manoj Kumar. 2013. Influence of Body Position on Severity of Obstructive Sleep Apnea: A Systematic Review. *International Scholarly Research Notices* 2013 (2013), e670381. <https://doi.org/10.1155/2013/670381>
- [76] David F Miranda, Angie S Lobo, Brooks Walsh, Yader Sandoval, and Stephen W Smith. 2018. New insights into the use of the 12-lead electrocardiogram for diagnosing acute myocardial infarction in the emergency department. *Canadian Journal of Cardiology* 34, 2 (2018), 132–145.
- [77] Anat Mirelman, Inbar Hillel, Lynn Rochester, Silvia Del Din, Bastiaan R. Bloem, Laura Avanzino, Alice Nieuwboer, Inbal Maidan, Talia Herman, Avner Thaler, Tanya Gurevich, Meir Kestenbaum, Avi Orr-Urtreger, Mirek Brys, Jesse M. Cedarbaum, Nir Giladi, and Jeffrey M. Hausdorff. 2020. Tossing and Turning in Bed: Nocturnal Movements in Parkinson's Disease. *Movement Disorders* 35, 6 (2020), 959–968. <https://doi.org/10.1002/mds.28006>

- [78] Rajalakshmi Nandakumar, Shyamnath Gollakota, and Nathaniel Watson. 2015. Contactless Sleep Apnea Detection on Smartphones. In *Proceedings of the 13th Annual International Conference on Mobile Systems, Applications, and Services*. Association for Computing Machinery, New York, NY, USA, 45–57. <https://doi.org/10.1145/2742647.2742674>
- [79] Ebrahim Nemati, M Jamal Deen, and Tapas Mondal. 2012. A wireless wearable ECG sensor for long-term applications. *IEEE Communications Magazine* 50, 1 (2012), 36–43.
- [80] Charn Loong Ng and Mamun Bin Ibne Reaz. 2016. Capacitive electromyography biosensor with wearable material as an insulator. In *2016 International Conference on Advances in Electrical, Electronic and Systems Engineering (ICAEEES)*. IEEE, 165–169.
- [81] Peter M Okin, Mary J Roman, Richard B Devereux, and Paul Kligfield. 1995. Gender differences and the electrocardiogram in left ventricular hypertrophy. *Hypertension* 25, 2 (1995), 242–249.
- [82] OpenBCI. 2024. *OpenBCI Shop*. Retrieved June 25, 2024 from <https://shop.openbci.com/products/cyton-biosensing-board-8-channel>
- [83] Sarah Ostadabbas, Maziyar Baran Pouyan, Mehrdad Nourani, and Nasser Kehtarnavaz. 2014. In-bed posture classification and limb identification. In *2014 IEEE Biomedical Circuits and Systems Conference (BioCAS) Proceedings*. IEEE, 133–136. <https://doi.org/10.1109/BioCAS.2014.6981663>
- [84] LD Ostrander Jr, RALPH L BRANDT, MARCUS O KJELSBERG, and FREDERICK H EPSTEIN. 1965. Electrocardiographic findings among the adult population of a total natural community, Tecumseh, Michigan. *Circulation* 31, 6 (1965), 888–898.
- [85] Dahat P, Toriola S, Satnarine T, Zohara Z, Adelekun A, Seffah KD, Dardari L, Salib K, Taha M, and Khan S. 2023. Correlation of Various Sleep Patterns on Different Types of Memory Retention: A Systematic Review. *Cureus* 15, 7 (2023), e42294.
- [86] Valerie Paasch, Teresa M Hoosier, Jennifer Accardo, Joshua B Ewen, and Keith J Slifer. 2012. Technical tips: performing EEGs and polysomnograms on children with neurodevelopmental disabilities. *The Neurodiagnostic Journal* 52, 4 (2012), 333–348.
- [87] D. Pani, A. Achilli, A. Spanu, A. Bonfiglio, M. Gazzoni, and A. Botter. 2019. Validation of Polymer-Based Screen-Printed Textile Electrodes for Surface EMG Detection. In *IEEE Transactions on Neural Systems and Rehabilitation Engineering*, Vol. 27. IEEE, 1370–1377. <https://doi.org/10.1109/TNSRE.2019.2916397>
- [88] Thomas Penzel, Marion Möller, Heinrich F Becker, Lennart Knaack, and Jörg-Hermann Peter. 2001. Effect of sleep position and sleep stage on the collapsibility of the upper airways in patients with sleep apnea. *Sleep* 24, 1 (2001), 90–95.
- [89] Philips. 2024. *Philips SmartSleep Deep Sleep Headband*. Retrieved June 1, 2024 from <https://www.usa.philips.com/c-e/smartsleep/deep-sleep-headband.html>
- [90] Maytus Piriyajitakonjj, Patchanon Warin, Payongkit Lakhan, Pitshaporn Leelaarporn, Nakorn Kumchaiseemak, Supasorn Suwanjakorn, Theerasarn Pianpanit, Nattee Niparnan, Subhas Chandra Mukhopadhyay, and Theerawit Wilaiprasitporn. 2020. SleepPoseNet: Multi-view learning for sleep postural transition recognition using UWB. *IEEE Journal of Biomedical and Health Informatics* 25, 4 (2020), 1305–1314.
- [91] Mehdi Ghalebeigy Poor, Hamidreza Ghasemi Bahraseman, Elnaz Pouranbarani, Reza Sarang, Mehdi Shafieian, and Karim Leilnahari. 2017. A comparative study in cervical muscle activities during various resting postures using electromyography. *American Journal of Biomedical Sciences* 9, 3 (2017).
- [92] M Baran Pouyan, Sarah Ostadabbas, Masoud Farshbaf, Rasoul Yousefi, Mehrdad Nourani, and MDM Pompeo. 2013. Continuous eight-posture classification for bed-bound patients. In *2013 6th International Conference on Biomedical Engineering and Informatics*. IEEE, 121–126. <https://doi.org/10.1109/BMEI.2013.6746919>
- [93] Inkscape Project. 2023. *Inkscape*. Retrieved June 23, 2024 from <https://inkscape.org>
- [94] Mustafa Radha, Pedro Fonseca, Arnaud Moreau, Marco Ross, Andreas Cerny, Peter Anderer, Xi Long, and Ronald M Aarts. 2019. Sleep stage classification from heart-rate variability using long short-term memory neural networks. *Scientific reports* 9, 1 (2019), 14149.
- [95] Tauhidur Rahman, Alexander T Adams, Ruth Vinisha Ravichandran, Mi Zhang, Shwetak N Patel, Julie A Kientz, and Tanzeem Choudhury. 2015. Dopplesleep: A contactless unobtrusive sleep sensing system using short-range doppler radar. In *Proceedings of the 2015 ACM international joint conference on pervasive and ubiquitous computing*, 39–50.
- [96] U. Rajendra Acharya, K. Paul Joseph, N. Kannathal, Choo Min Lim, and Jasjit S. Suri. 2006. Heart Rate Variability: A Review. *Medical and Biological Engineering and Computing* 44, 12 (2006), 1031–51. <https://doi.org/10.1007/s11517-006-0119-0>
- [97] Wietske Richard, Dennis Kok, Cindy den Herder, Martin Lamant, Harm van Tinteren, and Nico de Vries. 2006. The role of sleep position in obstructive sleep apnea syndrome. *Eur Arch Otorhinolaryngol* 263 (2006), 946–950. <https://doi.org/10.1007/s00405-006-0090-2>
- [98] Mahsan Rofouei, Mike Sinclair, Ray Bittner, Tom Blank, Nick Saw, Gerald DeJean, and Jeff Heffron. 2011. A Non-invasive Wearable Neck-Cuff System for Real-Time Sleep Monitoring. In *2011 International Conference on Body Sensor Networks*. 156–161. <https://doi.org/10.1109/BSN.2011.38>
- [99] Soha Rostaminia, Seyedeh Zohreh Homayounfar, Ali Kiaghadi, Trisha Andrew, and Deepak Ganesan. 2022. Phymask: Robust sensing of brain activity and physiological signals during sleep with an all-textile eye mask. *ACM Transactions on Computing for Healthcare (HEALTH)* 3, 3 (2022), 1–35.
- [100] Clodagh M Ryan and T Douglas Bradley. 2005. Pathogenesis of obstructive sleep apnea. *Journal of Applied Physiology* 99, 6 (2005), 2440–2450.

- [101] Youngsang Ryu, Sungbum Ju, Giduck Park, and HyunJeong Jang. 2011. Effects of bridging exercise methods on the muscular activity of the neck, trunk and lower limbs. *Journal of physical therapy science* 23, 6 (2011), 867–869.
- [102] Ibrahim Sadek, Edwin Seet, Jit Biswas, Bessam Abdulrazak, and Mounir Mokhtari. 2018. Nonintrusive Vital Signs Monitoring for Sleep Apnea Patients: A Preliminary Study. *IEEE Access* 6 (2018), 2506–2514. <https://doi.org/10.1109/ACCESS.2017.2783939>
- [103] Wilhelm Daniel Scherz, Daniel Fritz, Oana Ramona Velicu, Ralf Seepold, and Natividad Martínez Madrid. 2017. Heart Rate Spectrum Analysis for Sleep Quality Detection. *EURASIP Journal on Embedded Systems* 2017, 1 (2017), 26.
- [104] Qijia Shao. 2024. Weaving Physical and Physiological Sensing with Computational Fabrics. In *Proc. of MobiSys* (Minato-ku, Tokyo, Japan). Association for Computing Machinery, New York, NY, USA, 748–750. <https://doi.org/10.1145/3643832.3661385>
- [105] Qijia Shao, Jiting Liu, Emily Bejeraño, Ho Man Colman, Jingping Nie, Xiaofan Jiang, and Xia Zhou. 2024. Joey: Supporting Kangaroo Mother Care with Computational Fabrics. In *Proc. of MobiSys*. 237–251. <https://doi.org/10.1145/3643832.3661867>
- [106] Qijia Shao, Amy Sniffen, Julien Blanchet, Megan E. Hillis, Xinyu Shi, Themistoklis K. Haris, Jason Liu, Jason Lamberton, Melissa Malzkuhn, Lorna C. Quandt, James Mahoney, David J. M. Kraemer, Xia Zhou, and Devin Balkcom. 2020. Teaching American Sign Language in Mixed Reality. 4, 4, Article 152 (Dec. 2020), 27 pages. <https://doi.org/10.1145/3432211>
- [107] Fahmi Shibli, Jacob Skeans, Takahisa Yamasaki, and Ronnie Fass. 2020. Nocturnal Gastroesophageal Reflux Disease (GERD) and Sleep: An Important Relationship That Is Commonly Overlooked. *Journal of Clinical Gastroenterology* 54, 8 (2020), 663. <https://doi.org/10.1097/MCG.0000000000001382>
- [108] Ernst Simonson, HENRY BLACKBURN JR, Thomas C Puchner, Pauline Eisenberg, Fernanda Ribeiro, and Manuel Meja. 1960. Sex differences in the electrocardiogram. *Circulation* 22, 4 (1960), 598–601.
- [109] Carolyn M Sommerich, Sharon MB Joines, Veerle Hermans, and Samuel D Moon. 2000. Use of surface electromyography to estimate neck muscle activity. *Journal of Electromyography and kinesiology* 10, 6 (2000), 377–398.
- [110] Thekla Stefanou, David Guiraud, Charles Fattal, Christine Azevedo-Coste, and Lucas Fonseca. 2022. Frequency-domain sEMG classification using a single sensor. *Sensors* 22, 5 (2022), 1939.
- [111] Seeed Studio. 2025. XIAO ESP32C3. Retrieved April 27, 2025 from https://wiki.seeedstudio.com/XIAO_ESP32C3_Getting_Started/
- [112] MadeIRA USA. 2024. HC-12-SP Highly Conductive Embroidery Thread 12. Retrieved June 25, 2024 from <https://www.madeirausa.com/hc-12-sp-highly-conductive-embroidery-thread-12.html>
- [113] Alejandro Veiga, Laura Garcia, Lorena Parra, Jaime Lloret, and Vivian Augele. 2018. An IoT-based smart pillow for sleep quality monitoring in AAL environments. In *2018 Third International Conference on Fog and Mobile Edge Computing (FMEC)*. 175–180. <https://doi.org/10.1109/FMEC.2018.8364061>
- [114] Vincent Verhaert, Bart Haex, Tom De Wilde, Daniel Berckmans, Marie Vandekerckhove, Johan Verbraecken, and Jos Vander Sloten. 2011. Unobtrusive Assessment of Motor Patterns During Sleep Based on Mattress Indentation Measurements. *IEEE Transactions on Information Technology in Biomedicine* 15, 5 (2011), 787–794. <https://doi.org/10.1109/TITB.2011.2131670>
- [115] Olivia Walch, Yitong Huang, Daniel Forger, and Cathy Goldstein. 2019. Sleep stage prediction with raw acceleration and photoplethysmography heart rate data derived from a consumer wearable device. *Sleep* 42, 12 (2019), zsz180.
- [116] Zhaohua Wu and Norden E. Huang. 2009. Ensemble Empirical Mode Decomposition: A Noise-Assisted Data Analysis Method. *Advances in Adaptive Data Analysis* 1, 01 (2009), 1–41. <https://doi.org/10.1142/S1793536909000047>
- [117] Liping Xie, Zilong Li, Yihan Zhou, Yiliu He, and Jiaxin Zhu. 2020. Computational diagnostic techniques for electrocardiogram signal analysis. *Sensors* 20, 21 (2020), 6318.
- [118] Xiaowei Xu, Feng Lin, Aosen Wang, Yu Hu, Ming-Chun Huang, and Wenyao Xu. 2016. Body-Earth Mover’s Distance: A Matching-Based Approach for Sleep Posture Recognition. *IEEE Transactions on Biomedical Circuits and Systems* 10, 5 (2016), 1023–1035. <https://doi.org/10.1109/TBCAS.2016.2543686>
- [119] Xiaowei Xu, Feng Lin, Aosen Wang, Chen Song, Yu Hu, and Wenyao Xu. 2015. On-bed sleep posture recognition based on body-earth mover’s distance. In *2015 IEEE Biomedical Circuits and Systems Conference*. IEEE, 1–4. <https://doi.org/10.1109/BioCAS.2015.7348281>
- [120] Hongfei Xue, Wenjun Jiang, Chenglin Miao, Fenglong Ma, Shiyang Wang, Ye Yuan, Shuochao Yao, Aidong Zhang, and Lu Su. 2020. DeepMV: Multi-view deep learning for device-free human activity recognition. *Proceedings of the ACM on Interactive, Mobile, Wearable and Ubiquitous Technologies* 4, 1 (2020), 1–26.
- [121] Zhicheng Yang, PictureParth H. Pathak, PictureYunze Zeng, PictureXixi Liran, and PicturePrasant Mohapatra. 2017. Monitoring vital signs and postures during sleep using WiFi signals. *ACM Transactions on Sensor Networks* 13, 2 (2017), 14:1–14:32. <https://doi.org/10.1145/3051124>
- [122] Heenam Yoon, Suhwan Hwang, Dawoon Jung, Sangho Choi, Kwangmin Joo, Jaewon Choi, Yujin Lee, and Do-Un Jeong. 2015. Estimation of sleep posture using a patch-type accelerometer based device. In *2015 37th Annual International Conference of the IEEE Engineering in Medicine and Biology Society (EMBC)*. IEEE, 4942–4945. <https://doi.org/10.1109/EMBC.2015.7319500>
- [123] Shichao Yue, Yuzhe Yang, Hao Wang, Hariharan Rahul, and Dina Katabi. 2020. BodyCompass: Monitoring sleep posture with wireless signals. *Proceedings of the ACM on Interactive, Mobile, Wearable and Ubiquitous Technologies* 4, 2 (2020), 1–25.
- [124] Feng Zhang, Chenshu Wu, Beibei Wang, Min Wu, Daniel Bugos, Hangfang Zhang, and K. J. Ray Liu. 2021. SMARS: Sleep Monitoring via Ambient Radio Signals. *IEEE Transactions on Mobile Computing* 20, 1 (2021), 217–231. <https://doi.org/10.1109/TMC.2019.2939791>